REPORT NO.
EERC 76-16
JUNE 1976

EARTHQUAKE ENGINEERING RESEARCH CENTER

CYCLIC SHEAR TESTS OF MASONRY PIERS
VOLUME 2 — ANALYSIS OF TEST RESULTS

by

RONALD L. MAYES
YUTARO OMOTE
RAY W. CLOUGH

Report to the National Science Foundation
and the Masonry Institute of America

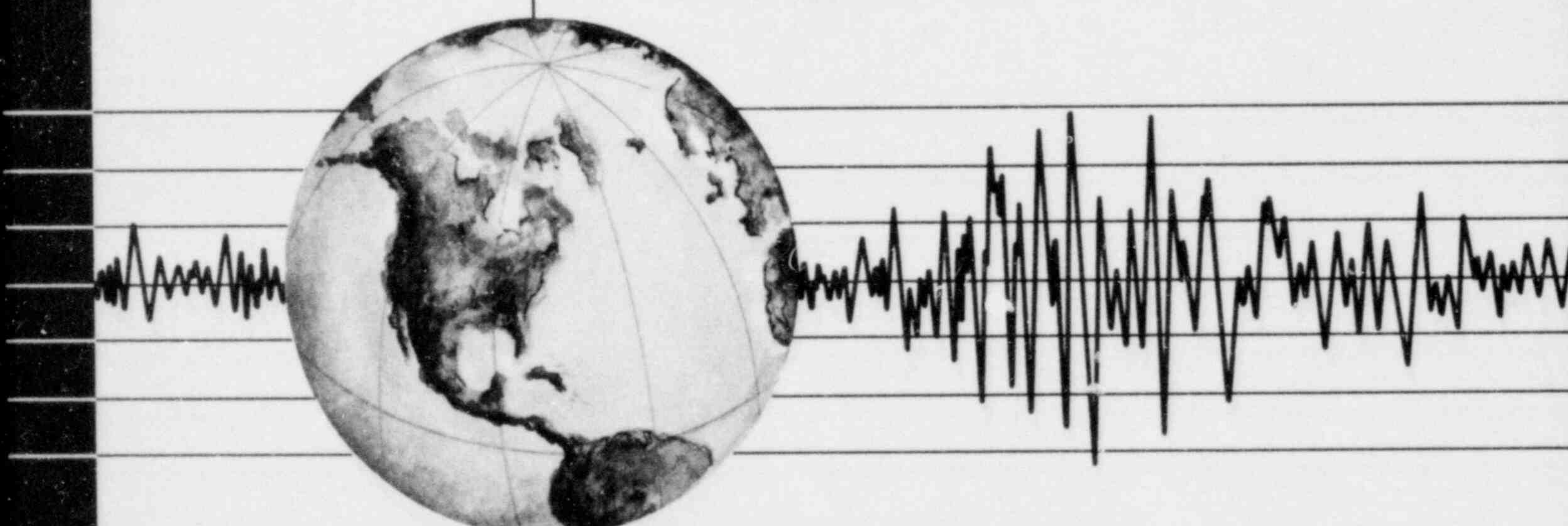

COLLEGE OF ENGINEERING

UNIVERSITY OF CALIFORNIA · Berkeley, California

CYCLIC SHEAR TESTS OF MASONRY PIERS
VOLUME 2 - ANALYSIS OF TEST RESULTS

by

Ronald L. Mayes

Yutaro Omote

and

Ray W. Clough

Report to

National Science Foundation

and

Masonry Institute of America

EERC Report No. 76-16

Earthquake Engineering Research Center

College of Engineering

University of California

Berkeley, California

June 1976

ABSTRACT

This report presents an analysis of the results of the tests described in the EERC Report No. 76-8. In Chapter 1, a comparison of the critical tensile strengths obtained from the double pier tests with those obtained from a simple diagonal compression test on a square panel is presented.

The report also contains idealized hysteresis envelopes developed from the experimental results for the two primary modes of failure observed in the test series. Also included in this chapter, are theoretical methods for calculating the ultimate shear and flexural capacities of the piers. The capacities obtained from the theoretical methods are compared with the experimental results; good agreement is obtained for the flexural capacity whereas the method used for the shear mode of failure overestimates the experimentally determined values.

Finally, comparison of the results obtained in this test program, with those of other investigations is given.

ACKNOWLEDGMENTS

This investigation was jointly sponsored by the National Science Foundation under Grant No. AEN 73-07732 and the Masonry Institute of America. The authors wish to thank Mr. W. L. Dickey, a consulting Structural Engineer of the Masonry Institute of America for the help and encouragement he has given as an industry consultant throughout the test program. Thanks are also due to Dr. P. Hidalgo and Professor H. McNiven for reviewing the manuscript and providing helpful comments, to S. W. Chen, J. Kubota, A. Shaban and A. Agarwal for their help in performing the tests and reducing the test data, and to Dr. B. Bolt for reviewing the manuscript.

The typing was done by Ms. Toni Avery and the drafting by Ms. Gail Feazell.

TABLE OF CONTENTS

LIST OF TABLES

LIST OF FIGURES

1. EFFECT OF TEST TECHNIQUE ON SHEAR STRENGTH

1.1 Introduction

One of the more important parameters required for the design of masonry structures is the shear strength of masonry walls. At present, most building codes use an allowable design shear strength for masonry that is related to the compressive strength, f'_m, of a prism. In the Uniform Building Code the allowable design shear strength for squat reinforced walls is $2.0 \sqrt{f'_m}$ with a maximum value of 60 psi for uninspected masonry and 120 psi for inspected masonry. Since it is possible for an assemblage with little or no shear strength to have a significant compressive strength, the authors conducted a secondary test program to examine an alternative method for the determination of the allowable shear strength of masonry walls.

The method selected for investigation has been used quite extensively in test programs performed by Blume[1], Borchelt[2], Degenkolb[3] and Yokel and Fattal[4] and is shown in Fig. 1.1. It was modified towards the end of the test program to give another method for use in this correlation study. The modified test setup is shown in Fig. 1.2.

The objective of the secondary test program was to obtain a correlation between the results obtained from simple diagonal compressive tests and those from the more realistic double pier tests. The parameter chosen to measure the correlation was the critical tensile strength. For each set of two double pier test specimens described in Volume 1[5] at least two 32 in. x 32 in. (81cm x 81cm) square shear panels were constructed with the same masonry units, grout and mortar and at the same time as the large double pier panels. For most of this secondary test program, only the test setup shown in Fig. 1.1 was available; the test setup shown in Fig. 1.2 was used only in conjunction with the last set of double pier tests.

The following two sections of this chapter describe the two diagonal compression test setups and the formulations used to determine the critical tensile strength of the test panels. The third section describes the formulation used to evaluate the critical tensile strength of the double pier tests while the fourth correlates the various sets of results.

1.2 Diagonal Compression Test

An overall view of the diagonal compression test setup is shown in Figs. 1.1 and 1.3. Top and bottom shoes to apply the loading were fabricated from 1 in. thick steel plates to form a 90 degree bearing corner which transferred the vertical compressive force to the panel. A four million pound Universal Testing Machine applied the load at a rate of approximately 8000 pounds per minute until failure. A typical failure of a test specimen is shown in Fig. 1.4.

Two different theoretical formulations have been used to calculate the critical tensile strength of the panels. The first was used by Borchelt[2] and assumed that the compressive load P applied a uniform shear stress along each side at the panel as shown in Fig. 1.5. The critical tensile strength, σ_{tcr}, was obtained from a Mohr's circle formulation applied at the center of the panel such that

$$\sigma_{tcr} = \sqrt{\tau^2 + \left(\frac{\sigma_c}{2}\right)^2} - \frac{\sigma_c}{2} \tag{1.1}$$

where σ_c is the applied compressive stress, and τ is the assumed shear stress given by

$$\tau = P/(\sqrt{2}A) \tag{1.2}$$

in which P is the applied compressive load and A is the area of one side of the square panel.

Blume[1] in his test program used a more exact formulation based on analytic and photoelastic studies performed by Frocht[6] on an homogeneous square panel. The critical tensile strength obtained from Blume's work is

$$\sigma_{tcr} = \sqrt{2.422\tau^2 + \left(\frac{\sigma_c}{2}\right)^2} - \left(0.832\tau + \frac{\sigma_c}{2}\right) \qquad (1.3)$$

where τ and σ_c are as defined above.

1.3 Modified Diagonal Compression Test or Simple Shear Test

Borchelt's formulation of Eq. (1.1) assumes a uniform shear force along each side of the panel. In order to induce this state of stress as accurately as possible the simple diagonal compression test arrangement was modified as shown in Fig. 1.2. The objective of the modification was to provide another test method capable of measuring the critical tensile strength. Inherent in this objective is acknowledgement of the fact that the complex state of stress induced at the corners of the panel in the simple diagonal compression test does not adequately represent Borchelt's assumed boundary force distribution shown in Fig. 1.5.

The initial test setup used for the modified shear test is shown in Fig. 1.2. One inch steel plates shown in Fig. 1.6 were attached to each face of the panel with epoxy cement and were connected by a 1-5/8 in. diameter hardened steel pin to the loading plates (see Fig. 1.7). The compressive load P applied to the top and bottom plates is transferred to the epoxied plates by the mechanism shown in Fig. 1.7, so that a shear force of $P/\sqrt{2}$ is applied to each side of the panel. To avoid instability in the loading mechanism it is imperative that the top and bottom loads P be perfectly aligned so that no external moment is applied to the panel.

Because of the time required to develop the modified test setup only one set of square panels was tested in this way. The mode of failure shown in Fig. 1.8 indicates that in addition to the expected diagonal crack a second crack was induced at the end of the loading plate. This was attributed to a slight rotation that occurred in the panel towards the end of the test sequence. To prevent this stress concentration the loading plates were then modified by the addition of the plate shown in Fig. 1.6. This revised test mechanism will be used for part of the follow up test program to be done on eighty single piers.

The critical tensile strength established with this loading mechanism corresponds to the formulation of Eq.(1.1).

1.4 Critical Tensile Strength of Double Pier Tests

In order to estimate the critical tensile strength of the piers that failed in the shear mode during the double pier test program [5] three assumptions were made: (1) A point of inflexion was assumed at the mid-height of the pier, (see Fig. 1.9). (2) Each pier was assumed to resist half of the applied shear load, and the shear stress distribution across the width of the panel was assumed to be parabolic. (3) The compressive load acting at the center of each pier was modified by the axial forces induced by the overturning moment acting on the panel, as shown in Fig. 1.9.

With these assumptions the critical tensile strength, σ_{tcr}, of the double pier was calculated from the stress state at the center of the pier by a Mohr's circle formulation similar to Eq.(1.1), such that

$$\sigma_{tcr} = \sqrt{(1.5\tau)^2 + \left(\frac{\sigma'_c}{2}\right)^2} - \frac{\sigma'_c}{2} \tag{1.4}$$

where

$$\tau = P/2A$$

is the average shear stress, P is the shear load applied to the full panel and A is the area of one pier. σ'_c is the modified compressive stress and equals $(F_b - \frac{Ph}{L})/A$, where F_b is the direct compressive load on one pier and h and L are defined in Fig. 1.9.

1.5 Discussion of Test Results

Each set of double pier panels and the associated square specimens were constructed and cured under the same conditions. All panels were constructed to the same specifications, as given in Volume 1 (5). Because each of the nine sets of panels were built at different times, the grout, mortar, and prism strengths varied according to normal workmanship; the measured values are given in Table 2.1 of Volume 1.

The results of all simple diagonal compressive tests performed on the square specimens are given in Table 1.1. Both the shear stress obtained from Eq.(1.2) and the critical tensile strength obtained from Eq.(1.3) are tabulated. The range of the critical tensile strength is from 181 psi to 316 psi with an average value of 257 psi and a standard deviation of 60 psi. For the purpose of comparison, the maximum standard deviation obtained from four identical panels in the extensive Blume test program on clay brick square panels tested in a similar manner was 48.6 psi.

The critical tensile strength of the double pier panels obtained from Eq.(1.4) is given in Table 1.1. The range of the values is 116 psi to 386 psi with an average value of 228 psi and a standard deviation of 75 psi. A comparison of the average values of the critical tensile strengths (228 psi and 257 psi) from the two different types of tests is encouraging. However, when the range of the results and the standard deviations are considered, a wide scatter of values is evident.

To compare the results of tests performed on corresponding panels, the quantity designated Ratio 1 of Table 1.1 was computed by taking the ratio of the critical tensile strength of the square panel to the critical tensile strength of the double pier panel. This ratio varied from 0.70 to 1.97, with eight of the thirteen test ratios being within ± 35 percent of the value of one. Ratio 2 of Table 1.1 was computed by taking the ratio of the average value of the critical tensile strength of all square panels (257 psi) to the critical tensile strength of each double pier panel. In this case the ratio varied from 0.67 to 2.20 with nine of the thirteen test values being within ± 33 percent of one.

The only two tests performed with the modified mechanism of Fig. 1.2 gave a critical tensile strength of 156 psi which is considerably lower than the average value (257 psi) obtained with the original system. However, as was noted earlier both test panels tended to rotate slightly towards the end of the test and failure may have been induced by this rotation.

Because the objective of the series of tests reported in this chapter was to examine alternative simplified methods of determining the shear strength of masonry walls, the authors are encouraged by the comparison of the average values of the critical tensile strengths obtained from double pier and simplified tests; at the same time, however, they are disturbed by the wide scatter of the results. Both of the test methods described in Sections 1.2 and 1.3 will be used in a follow up study on eighty single pier specimens, and at the conclusion of this extensive test series it is hoped that a more reliable simplified test method of evaluating the shear strength of walls can be recommended.

TABLE 1.1

COMPARISON OF CRITICAL TENSILE STRENGTHS FROM DOUBLE PIER AND DIAGONAL COMPRESSION TESTS

Test No.	Double Pier Tests: Frequency (cps)	Vertical Re-bar	Horizontal Re-bar	Bearing Stress (psi)	Ultimate Shear Stress (psi)	Critical Tensile Strength from Eqn.1.4 (psi)	Diagonal Compression Tests: Ultimate Shear Stress of Square Panels (psi) Eqn. 1.2	Average Ultimate Shear Stress (psi)	Average Critical Tensile Strength Eqn.1.3 (psi)	Ratio 1 see Note 1	Ratio 2 see Note 2
1	0.02	2-#6	---	250	135	160	406	409	300	1.87	1.60
2	3	2-#6	---	250	173	249	413			1.20	1.03
3	0.02	2-#4	---	125	142	234	331	431	316	1.35	1.10
4	3	2-#4	---	125	135	197	530			1.60	1.30
5	0.02	2-#6	---	0	107	232	369	357	262	1.13	1.10
6	3	2-#6	---	0	133	284	345			0.92	0.90
7	0.02	2-#6	3-#5	250	212	318	400 467 388	417	306	0.96	0.85
8	3	2-#6	3-#5	250	252	386				0.79	0.67
9	0.02	2-#6	---	500	154	116	336	312	229	1.97	2.20
10	3	2-#6	---	500	178	130	287			1.76	1.97
13	0.02	2-#4	3-#7,2-#5	125	151	259	278	247	181	0.70	0.9[illegible]
14	3	2-#4	3-#7,2-#5	125	150	257	215			0.70	1.00
17	3	---	---	250	123	142	246 270	258	189	1.33	1.81
						$\bar{x}$ = 228 σ = 75	$\bar{x}$ = 352 σ = 82		$\bar{x}$ = 257 σ = 60		

NOTES:

(1) Ratio 1 is the ratio of Average Critical Tensile Strength of the square panels obtained from Eq. 1.3 to the Critical Tensile Strength of the corresponding double piered panel obtained from Eq. 1.6.

(2) Ratio 2 is the ratio of the Average of the Critical Tensile Strengths of all square panels (257 psi) to the Critical Tensile Strength of the double piered panel.

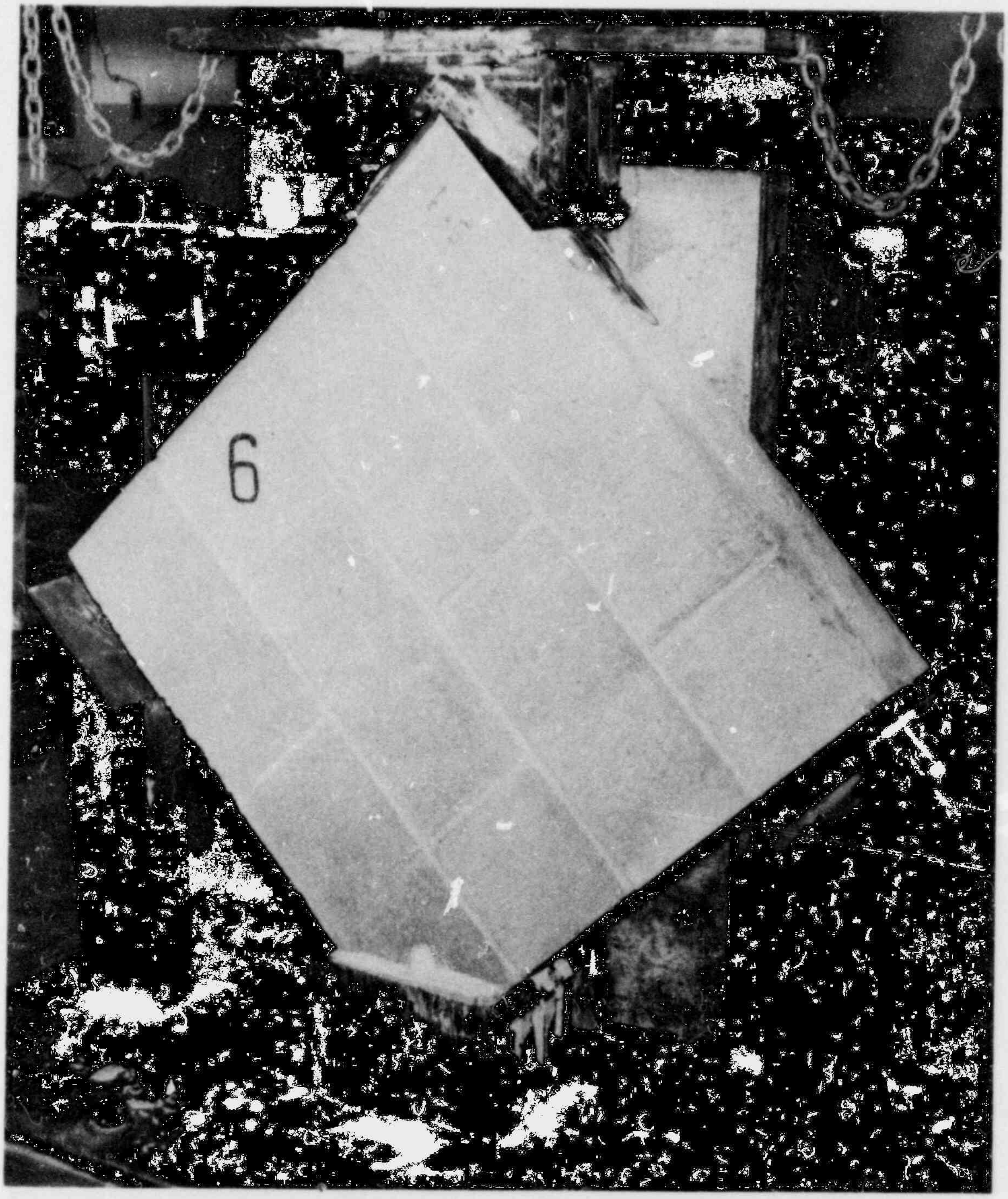

FIG. 1.1 OVERALL VIEW OF DIAGONAL COMPRESSION TEST SETUP

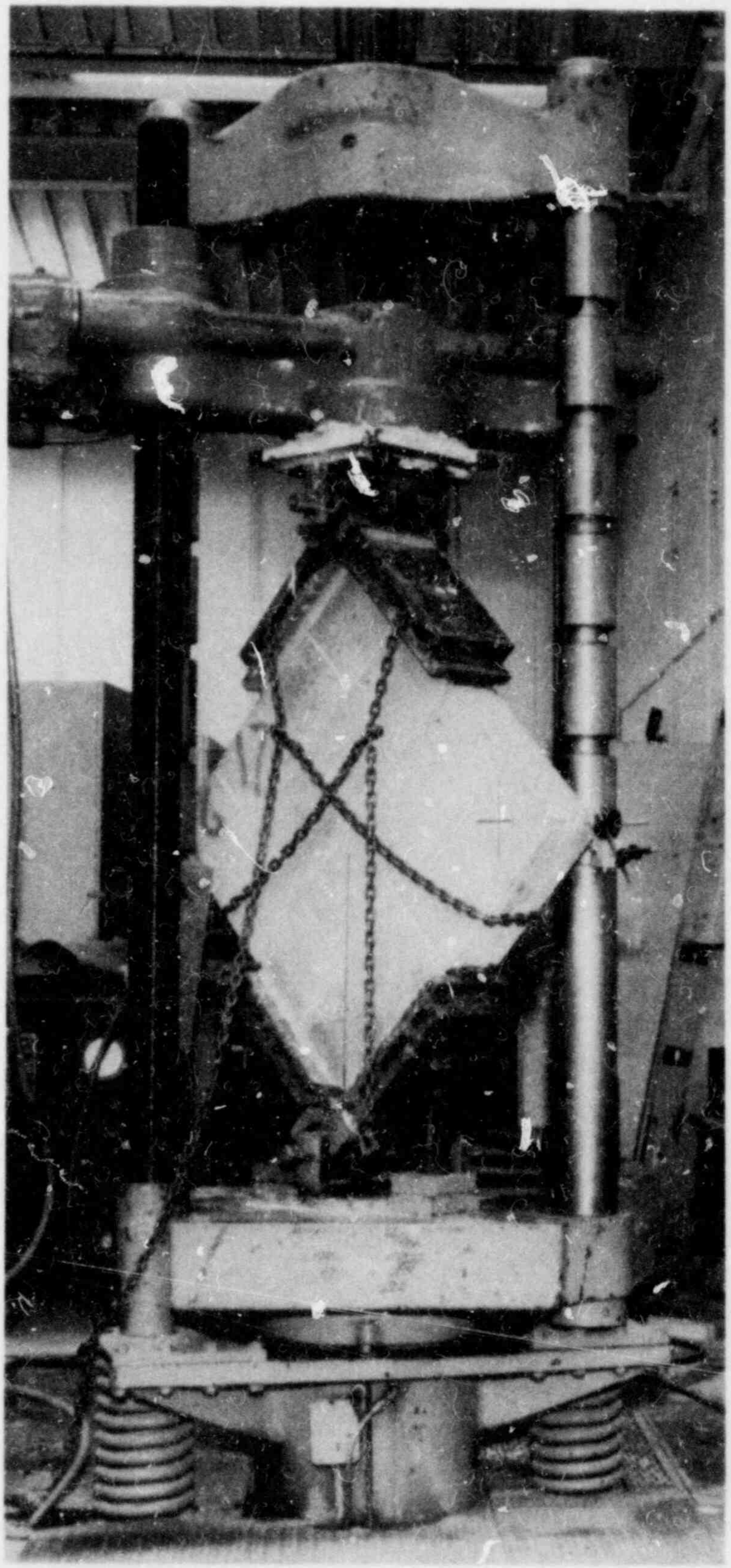

FIG. 1.2 OVERALL VIEW OF MODIFIED DIAGONAL COMPRESSION TEST SETUP

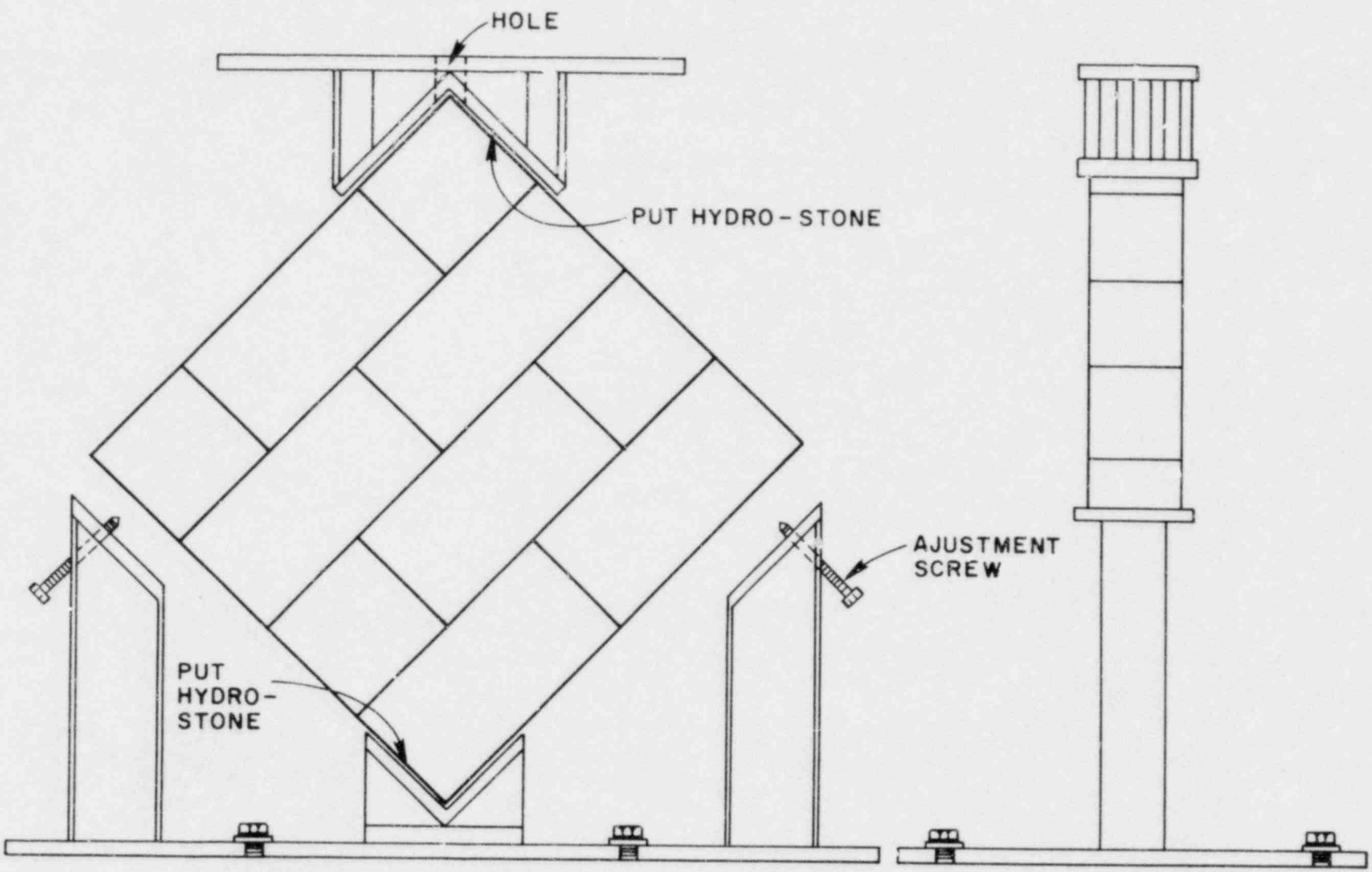

FIG. 1.3 DIAGONAL COMPRESSION TEST SETUP

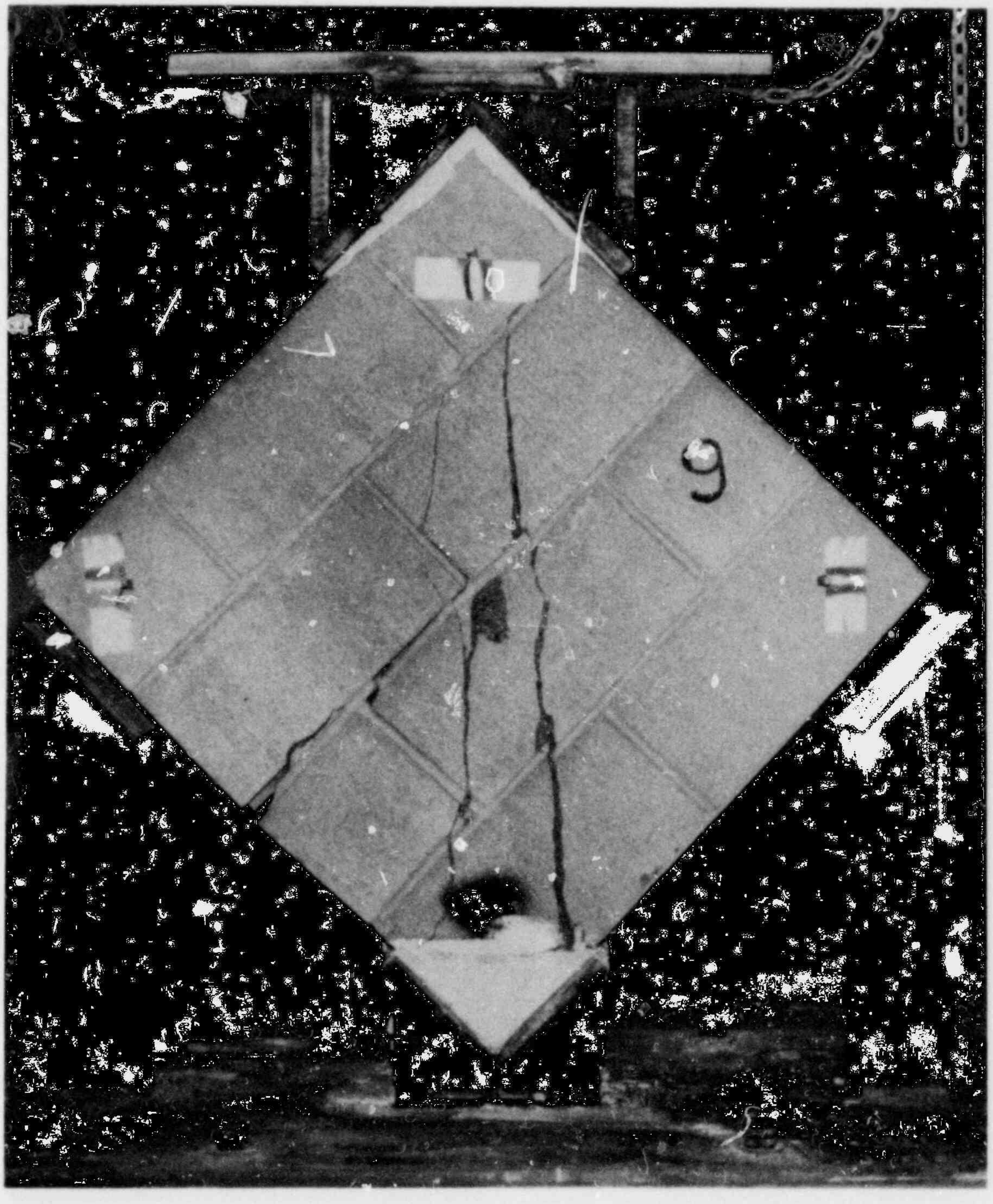

FIG. 1.4 TYPICAL FAILURE OF DIAGONAL COMPRESSION TEST

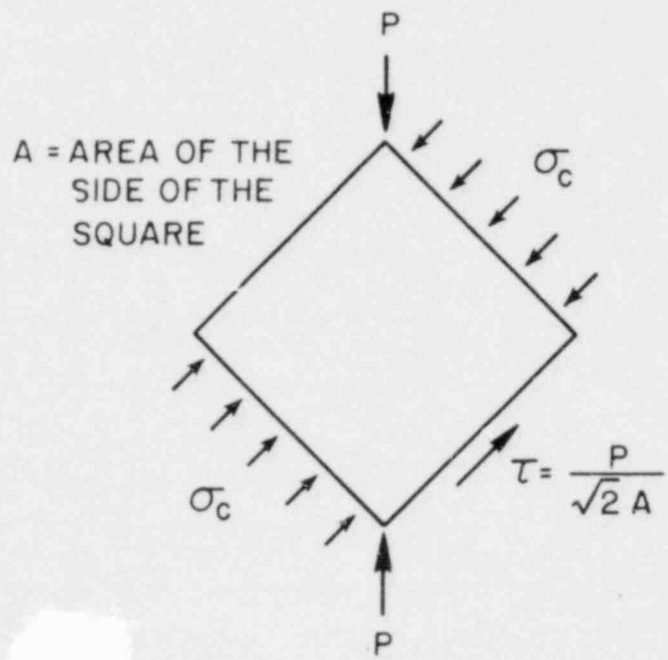

FIG. 1.5 ASSUMED STRESS DISTRIBUTION OF BCRCHELT'S TESTS

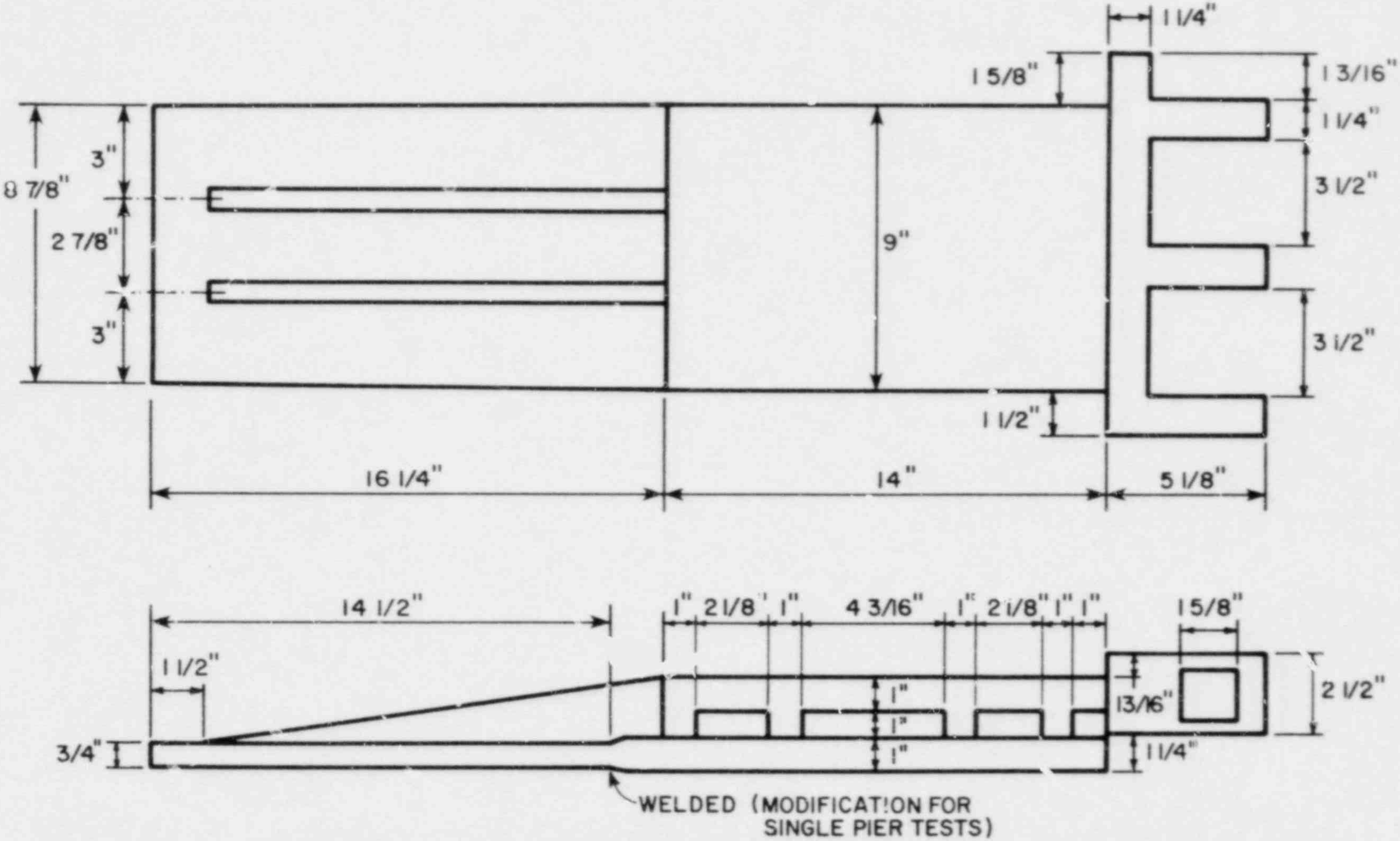

FIG. 1.6 PLATES USED FOR MODIFIED TEST SETUP

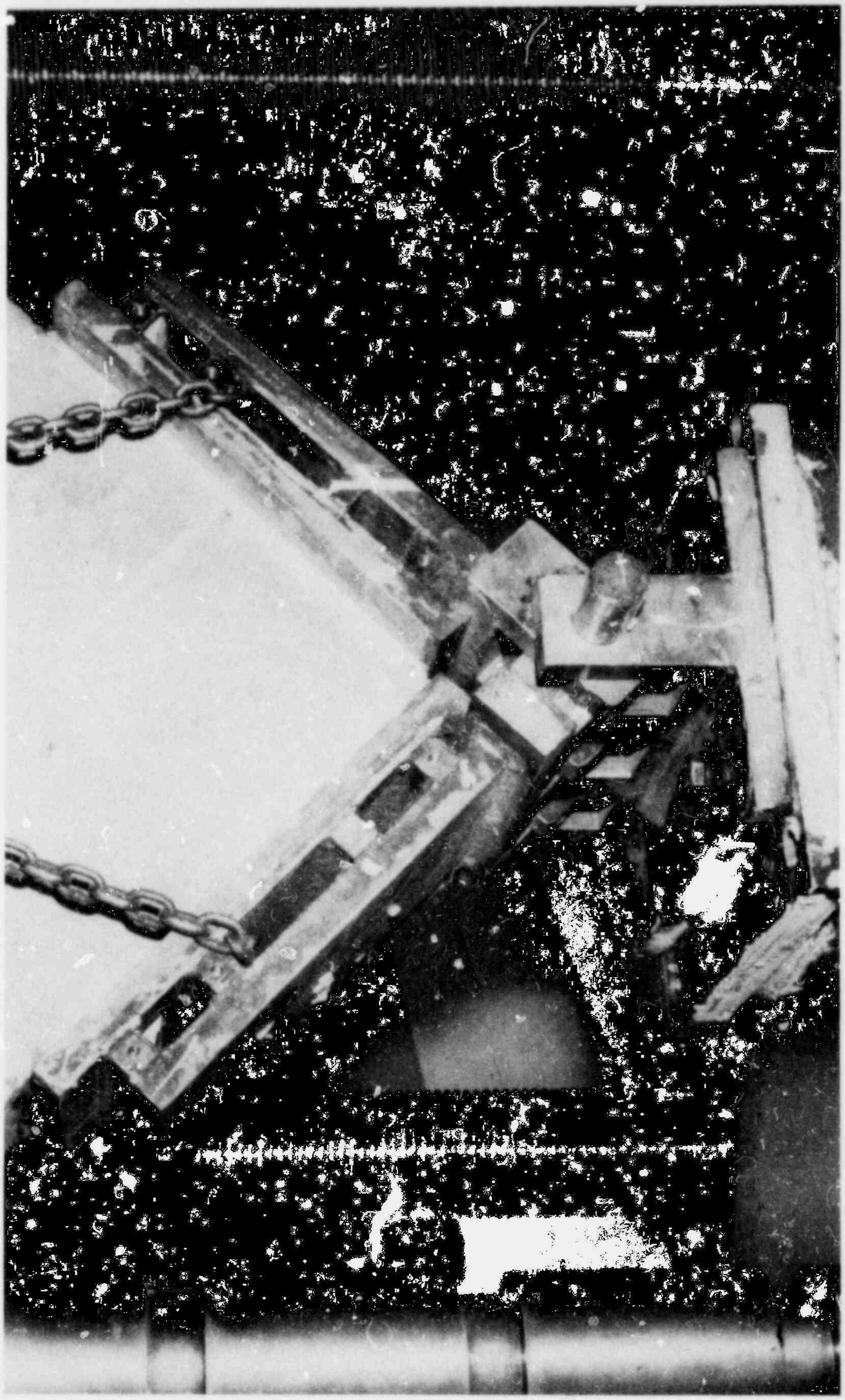

FIG. 1.7 CLOSE VIEW OF MODIFIED TEST SETUP

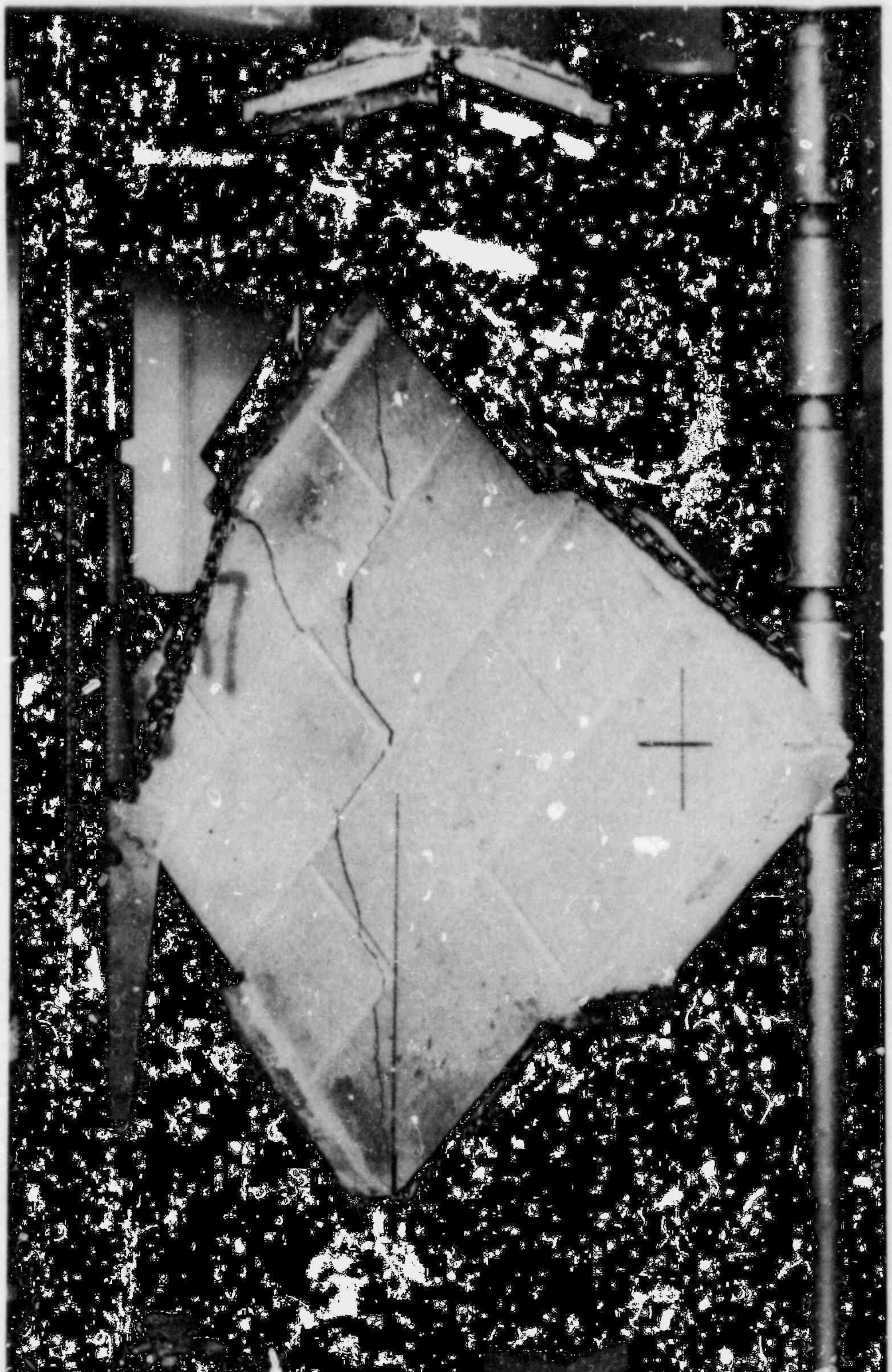

FIG. 1.8 MODE OF FAILURE OF MODIFIED DIAGONAL COMPRESSION TEST

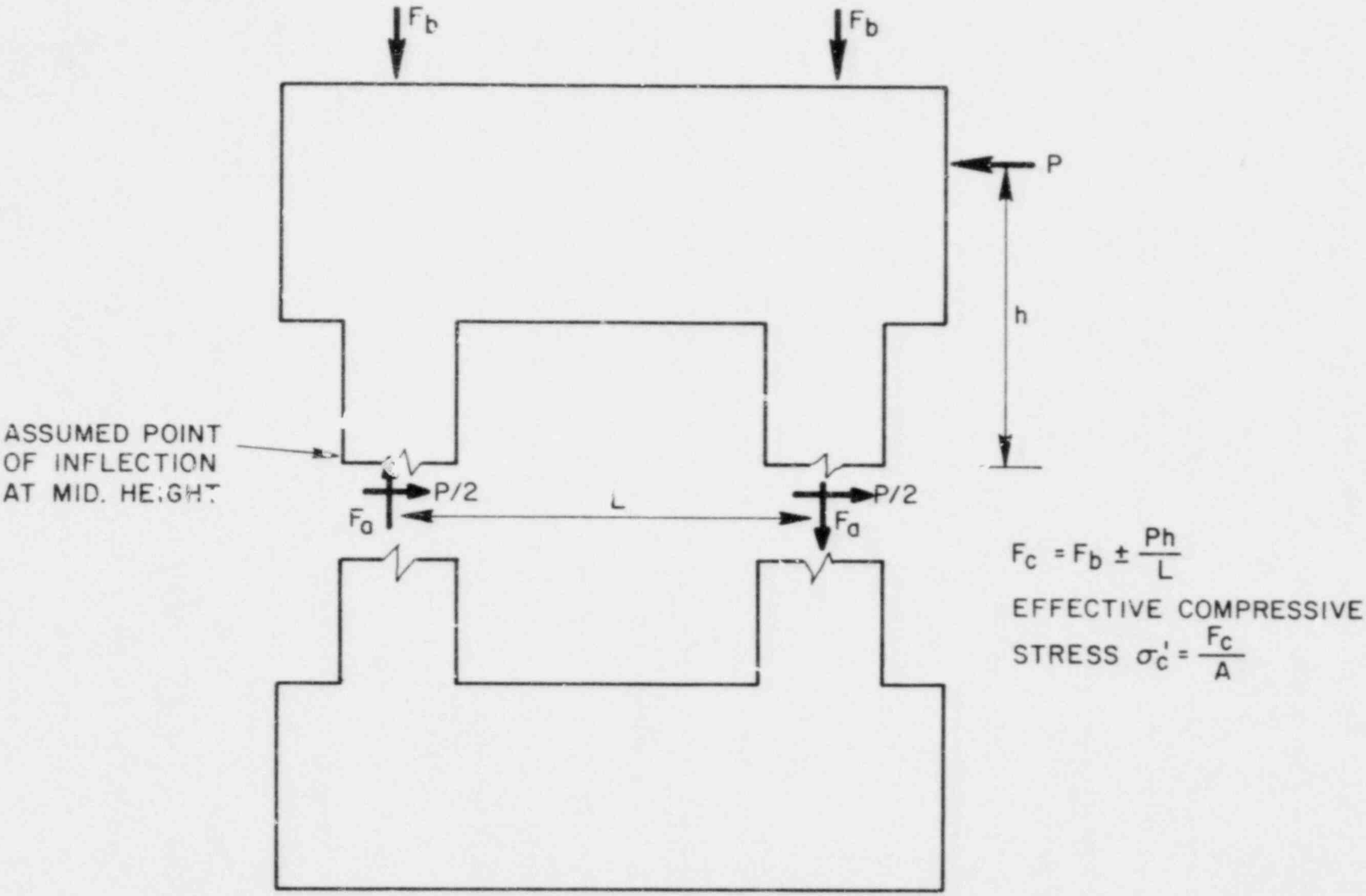

FIG. 1.9 ASSUMED FORCE DISTRIBUTION IN DOUBLE PIER TESTS

2. IDEALIZED HYSTERESIS ENVELOPES FOR THE DOUBLE PIERS

2.1 Introduction

The ultimate objective of the ongoing masonry research program of which this test series is a part, is to develop the capability of performing an inelastic response analysis of multistory masonry buildings subjected to earthquake ground motion. The approach being followed is similar to that used for reinforced concrete and steel buildings. That is, the inelastic behavior of typical structural components is determined experimentally and from these experimental results idealized inelastic models are developed which adequately describe the behavior of the components. At a later date the models will be incorporated into an inelastic analysis computer program thus enabling the ultimate objective to be achieved.

The objective of this chapter is to present models of the hysteresis envelopes determined from the experimental behavior of the piers observed in the test series described in Volume 1 of this report(5). The piers had a height to width ratio of two, and until additional tests are performed on piers with other height to width ratios the models presented herein can be considered valid only for these piers. Furthermore, the hysteresis envelopes are idealized from a displacement controlled test of gradually increasing magnitude; therefore, future tests are necessary to validate these results for loading that is more random in nature.

In idealizing the experimental curves, several variables must be evaluated from the test results. These include the envelopes of the hysteresis loops, the ultimate or maximum strength of the pier and the stiffness parameters defining the various stages of the hysteresis envelopes. Each step in the idealization process is discussed in the following sections of this chapter. The final step will be the development of a set of curves to model the actual cyclic behavior, but this will be done after the single pier test program has been completed.

2.2 Shape of Idealized Hysteresis Envelopes

The first step in developing a model for the hysteretic behavior of the piers is to develop the hysteresis envelope. The experimental hysteresis envelopes for the seventeen piers are presented in Figs. 4.37 to 4.40 of Volume 1. Figure 4.36 of that report also identifies four classifications for the modes of failure observed in the tests. These include the shear mode of failure (A) observed in Tests 1, 2, 5, 6, 7, 8, and 17; the shear mode of failure with vertical cracks (A'), observed in Tests 9-12; the combined shear and flexural mode of failure (B) observed in Tests 3 and 4; and the flexural mode of failure (C) observed in Tests 13-16. Two models for the hysteresis envelopes are developed to represent the four types of failure modes, since the model for shear failure modes A, A' and B are similar, with the only difference being the ductility developed at the maximum load. The proposed hysteresis envelopes for the two models are presented in a general format and then the stiffness parameters associated with various sections of the envelopes are determined from the experimental curves.

2.2.1 General Form of the Idealized Hysteresis Envelopes

(a) Shear Mode of Failure - Types A, A' and B

This envelope form is presented in Fig. 2.1(A) and is the simpler of the two. The initial stiffness indicated by line OA is K_{el}; this is maintained until 50 percent of the peak ultimate strength is attained at a displacement d_1. This segment of the model envelope is introduced to simulate the stiffness of the pier in the low load region. As may be seen in Figs. 4.42 and 4.43 of Volume 1, the stiffness degradation from 0 to 0.5 P_u is substantial and any attempt to idealize the stiffness in this range will produce a wide scatter of results when compared with experimental results. However, it is important that the idealized model have a reasonable approximation to the pier stiffness properties in this region. Segment AB has a stiffness of K_{e2} and this is maintained until 90 percent of the peak ultimate strength is attained at a displacement d_2. The segment BC represents the portion of the curve over which the maximum load is maintained. The ratio d_4/d_2 is equivalent to the ductility indicators δ_1 and δ_2 associated with the average peak load described on page 51 of Volume 1[5]. Line CD intersects the displacement axis at d_5. The major difference among failure modes A, A' and B is the magnitude of the ratio d_2/d_4 and d_5. From Table 4.1 of Volume 1, d_2/d_4 ranges from 1.45 to 1.85 for A and B and 2.1 to 5.1 for A'. Furthermore, d_5 for A is between 0.7 and 1.0, it is approximately 0.8 for B and it ranges between 0.45 and 0.55 for A'.

(b) Flexural Mode of Failure - Type C

This envelope form is presented in Fig. 2.1(B). The initial segment of the curve 0A has a stiffness K_{e1} which is maintained up to a load P_{BC} at which flexural cracks occur at the toes of the piers. These cracks are due to a bond failure caused by moment induced tensile stresses at the toes. The stiffness then decreases to K_{e2} for the segment AB. K_{e2} defines d_2 by its intersection with a load of 0.9 P_y, where P_y is the flexural yield load discussed in Section 2.3. The stiffness then changes to K_{e3} for the portion of the curve BC between

$0.9\ P_y$ and $1.0\ P_y$. Segment CD represents the portion of the curve over which the maximum load is maintained, and the curve DE intersects the displacement axis at d_5.

The format of the preceding idealized hysteresis envelopes is presented in a manner such that they could be generated for piers for which no tests have been performed. In order to do this, values of P_u, the various K_e values, d_5 and ratios d_2/d_4 or d_3/d_4 would have to be established either by calculation or from data generated from experiments. Section 2.3 discusses the comparison between theoretical and experimental values of P_u and the following section presents experimentally determined values of K_e.

2.2.2 Stiffness Parameters of Idealized Hysteresis Envelopes

The three stiffness parameters K_{e1}, K_{e2} and K_{e3} defined in Fig. 2.1 are important in defining the shape of the hysteresis envelope. Furthermore, together with their corresponding loads they define the displacements d_1, d_2 and d_3. The objective of this section is to determine from the test results the various K_e/K_o ratios of Fig. 2.1 (A) and (B) where K_o is the initial stiffness of the pier calculated assuming the pier is fixed against rotation at both top and bottom.

As illustrated in Table 5.1 (page 78) of Volume 1, the range of the measured stiffness at an applied shear stress of 20 psi for the fully grouted walls is 415 to 605 kips/in. with an average value of 488 kips/in. If the piers are assumed to be fixed at the top and bottom such that the point of inflexion is at the mid-height of the piers, the total deflection Δ due to an applied load P may be estimated from

$$\Delta = \frac{PH^3}{12EI} + \frac{1.2PH}{GA} \qquad (2.1)$$

where H is the height of the pier, E and G are the elastic and shear moduli, respectively, I is the moment of inertia and A the cross sectional area. The average value of E obtained from uniaxial prism tests was 1.14×10^6 psi. If Poisson's ratio is assumed to be 0.15 then $G = 0.5 \times 10^6$ psi. The initial elastic stiffness K_o calculated from these easily measured properties is

$$K_o = \frac{P}{\Delta} = \frac{1}{\frac{H^3}{12EI} + \frac{1.2H}{GA}} = 464 \text{ kips/in.} \qquad (2.2)$$

where H = 64 in., d = 5.625 in. and b = 31.625 in. For the partially grouted piers (Test Nos. 11, 12), the center two cores are ungrouted and the corresponding calculation gives K_o = 392 kips/in

For comparison the average value of K_I, the stiffness indicator obtained from the fully grouted test results at an applied shear stress of 20 psi was 488 ksi (Table 5.1, Volume 1, Tests 1-10 and 13-16). The average value of K_I for the partially grouted test results at an applied shear stress of 20 psi was 425 kips/in. (Table 5.1, Volume 1, Test 11 and 12). Thus, the calculated values are within 5 percent of the average of the experimental values for the fully grouted piers and 8 percent for the partially grouted piers.

The idealized hysteresis envelope for the shear mode of failure shown in Fig. 2.1(A) contains two stiffness parameters, K_{e1} and K_{e2}, associated with the loads 0.5 P_u and 0.9 P_u, where P_u is the maximum ultimate shear load. The stiffness K_{e1} associated with the load 0.5 P_u was determined from Fig. 4.43 of Volume 1 at 0.25 P_u. The value of 0.25 was chosen because the stiffness degradation from zero up to 0.5 P_u is almost linear and therefore, the value at 0.25 P_u is a reasonable average of the values between the loads of 0 and 0.5 P_u. The value of K_{e2} was also determined from Fig. 4.43 of Volume 1 at a value of 0.9 P_u. The values of the ratios K_{e1}/K_o, K_{e2}/K_o and d_4/d_2, and the displacements d_5 which were also from the test results of Fig. 4.43 of Volume 1 are listed in Table 2.1.

As expected for this mode of failure there is significant variation in all the tabulated values. Before an average of these variables is used in a computer model to determine the overall response of a building to earthquake ground motion, a sensitivity study would have to be performed to determine what effect the range of each variable has on the overall building response.

The average value of each variable is given at the bottom of each column. Moreover, the average stiffness is also given with the results of Tests 9 and 10 removed; and the average ductility is given when Tests 11 and 12 are removed. This was done because Tests 9 and 10 had stiffness values much greater than all other tests, whereas Tests 11 and 12 had ductility values much greater than all other tests.

The idealized hysteresis envelope for the flexural mode of failure (Tests 13-16) shown in Fig. 2.1(B) contains three stiffness parameters K_{e1}, K_{e2} and K_{e3} associated with three loads P_{BC}, 0.9 P_y and P_y. P_{BC} is the load at which flexural cracking occurs at the toes of the piers due to a bond failure caused by moment induced tensile stresses, and P_y is the flexural yield load of the pier and is discussed in Section 2.3. The values of the three stiffness parameters, the ratios K_{e1}/K_o, K_{e2}/K_o, K_{e3}/K_o and d_4/d_3 as well as the displacement d_5 are given in Table 2.2.

The ranges of the variables associated with this mode of failure are not nearly as great as those for the shear mode of failure and, hence, a model based on the average values given at the bottom of the respective columns should be reasonably accurate.

2.3 Methods of Predicting Shear and Flexural Strength

To determine the ultimate strength of a particular test specimen or subassemblage, the strength associated wi h each possible mode of failure must be calculated. The mode of failure with the lowest strength will govern the ultimate strength and failure mechanism of the subassemblage.

The state of the art report by Mayes and Clough [28] presented several methods of evaluating the shear strength of a wall or pier. Each of these methods assumed the shear strength to be affected by certain primary variables: compressive load, aspect ratio, amount of reinforcement, mortar strength and tensile strength of the combined materials. Each of the theoretical and empirical relationships given for predicting the strength in shear [1, ?, 7, 13, 21-24, 29] possesses different degrees of accuracy. In contrast, the methods suggested for predicting the strength in flexure [7, 10, 14, 17, 18, 28, 29] were similar and reasonably accurate, and were based on methods commonly used for reinforced concrete flexural elements. The method selected here for evaluating the ultimate strength in the shear mode of failure is based on the critical tensile strength of the element. The method used for predicting the strength in the flexural mode of failure requires knowledge of the yield strength of the vertical reinforcement and is similar to that used by others.

2.3.1 Strength in the Flexural Mode of Failure

In order to determine the flexural capacity of the double pier panel, a point of inflexion is assumed at the mid-height of the piers and the compressive load at the center of each pier is modified by the axial forces induced by the overturning moments, (Fig. 1.9). A flexural mode of failure assumes yielding of the vertical reinforcement which in this case is at the jambs of each pier.

The mechanism of the flexural mode of failure can be explained with the aid of Fig. 2.2. The strain diagram of a pier is shown in Fig. 2.2(a) and the stress-strain curve of the steel is shown in Fig. 2.2(b). As the vertical steel yields the strain ε_s of Fig. 2.2(a) gradually increases with a resultant decrease in the area of masonry under compression. The limiting state is attained when the area of masonry under compression is unable to resist the compressive forces required for equilibrium at Section AA of Fig. 2.2(a). The steel strain at this limit state will be between ε_y and ε_u and therefore the stress in the vertical reinforcement will be between f_y and f_{ult}.

From the free body diagram shown in Fig. 2.3, taking moments about A and A' separately and then adding them, the flexural capacity of the panel is

$$\left(P_1+P_2\right)\frac{H}{2} = A_s f_y b' + \left(N + \frac{Ph_1}{L}\right)\frac{b}{2} + A_s f_y b' + \left(N - \frac{Ph_1}{L}\right)\frac{b}{2} . \qquad (2.3)$$

Therefore,

$$P_y = \frac{4}{H}\left[A_s f_y b' + \frac{b}{2} N\right] . \qquad (2.4)$$

If the ultimate stress of the steel is used, then

$$P_u = \frac{4}{H} \left[A_s f_{ult} b' + \frac{b}{2} N \right] . \qquad (2.5)$$

It should be noted that the steel in both piers would not be expected to reach the ultimate stress at the same time because of the differences in the vertical load.

These formulae assume that the moments resulting from the compressive stress block with the strain distribution of Fig. 2.1(a) are negligible.

The values of P_y and P_u were obtained from Eqs. (2.4) and (2.5) and are presented in Table 2.3 for Tests 3, 4, 7, 8 and 13-16. The values given in the table are half the loads (P_y and P_u of Eqs. (2.4) and (2.5)) applied to the full panel. This is consistent with the results presented in Table 4.1 of Volume 1, in which it is assumed that each pier resists half of the applied load. It is clear from Eq. (2.3) and Fig. 2.3 that this is not the case when the flexural capacity of the pier is calculated since the pier with the greater compressive load resists a larger lateral load. However, because the applied load is cyclic, comparisons of experimental and theoretical values based on half the total load (P_y and P_u of Eqs. (2.4) and (2.5)) are valid.

A comparison of the experimental and theoretical values for each of the tests is also presented in Table 2.3. It was noted in Volume 1 that Tests 3 and 4 failed in a combination of the shear and flexural modes of failure, and that Tests 7 and 8 had ultimate shear strengths significantly greater than the horizontally unreinforced panels. The comparison of the experimental ultimate load (P) of Tests 3 and 4 with the theoretical yield load (P_y) indicates that the piers never quite attained their flexural capacity and therefore should be considered to have failed in the shear mode. A similar comparison for Tests 7 and 8 indicates that the piers only attained 50 percent of their flexural capacity and thus their increase in shear strength is due solely to the effect of horizontal reinforcement.

The ratio $\frac{P}{P_y}$ for Tests 13 and 14 indicates that the piers almost attained their flexural capacity and because diagonal shear cracks did not form in the piers, it can be assumed that they exhibited a flexural mode of failure.

The ratio $\frac{P}{P_y}$ for Tests 15 and 16 (which contained plates in the mortar joints at the toes of the piers) indicates that significant yielding of the vertical reinforcement occurred. The ratio $\frac{P}{P_u}$ was 0.95, indicating that the vertical reinforcement almost reached its ultimate stress f_u. This is consistent with the assumption stated after Eq. (2.5).

In summary, the method used for calculating the flexural capacity of the piers was capable of defining both the yield and ultimate flexural capacity of the piers, and the comparison with the experimental results indicates good agreement. This is consistent with the conclusions of other investigators.

2.3.2 Strength in the Shear Mode of Failure

Several theoretical and empirical relationships are available in the literature(1, 2, 7, 13, 21-24, 29) for predicting the ultimate strength of piers in the shear mode of failure. Each possesses different degrees of accuracy and generally contains a significant amount of scatter in correlation with experimental results. Several different test techniques were used in the development of these methods and most of the test specimens considered were unreinforced. The availability of several different methods indicates both the difficulty of the prediction and the lack of an accepted method for predicting the ultimate shear strength of a masonry pier.

One of the major questions arising from the double pier test results, as well as from studies performed by others, concerns the effect of horizontal reinforcement on the ultimate strength in the shear mode of failure. It is clear that horizontal reinforcement is not effective until micro or major diagonal cracking has occurred; however, the principal question is to determine how the reinforcement and masonry pier interact after the initial crack has developed. A summary of results presented in the state of the art report by Mayes and Clough[28] indicates that there is no correlation between shear strength and the amount of horizontal reinforcement. However, Priestley and Bridgeman's[18,27] extensive study on cantilever piers indicates that a sufficient amount of horizontal reinforcement can completely suppress the shear mode of failure. Because of the lack of consistency in the test results available to date the effect of horizontal reinforcement on the shear mode of failure will be extensively studied in the single pier test program.

The methodology being evaluated for calculating the ultimate strength in the shear mode of failure (to be used in this and later in the single pier test program) is based on the critical tensile strength of square panels. The method has been presented and discussed in Chapter 1, where a comparison of the critical tensile strengths obtained from the piers and the small square panels is presented. It should be noted, however, that the method as presented in Chapter 1 does not account for the effect of horizontal reinforcement.

Equation (1.4) of Section 1.4 presents a formula for calculating the critical tensile strength of piers failing in shear based on the results of the double pier tests. The assumptions used in this derivation are discussed in Section 1.4. By rearranging Eq. (1.4) a formula for calculating the ultimate shear strength of a pier can be derived as a function of the applied compressive load and the critical tensile strength of the pier. In this method the critical tensile strength is obtained from the square panel tests described in Section 1.2. The formula is

$$\tau = \sqrt{\frac{1}{1.5}\left(\sigma_{tcr}^{2} + \sigma_{tcr}\sigma_{c}'\right)} \tag{2.6}$$

where τ is the ultimate shear stress of a single pier of the double pier panel, σ_c' is the compressive stress and σ_{tcr} is the critical tensile stress obtained from the square panel tests. For the double pier tests σ_c' is a function of both the initial applied compressive stress σ_c and the applied lateral load as shown in Fig. 1.9.

$$\sigma_c' = \frac{F_b}{A} \pm \frac{Ph}{AL} \tag{2.7}$$

where P is the lateral load applied to the panel. In terms of the critical single pier

$$\sigma_c' = \sigma_c - 2\tau \frac{h}{L} \tag{2.8}$$

Therefore, to solve Eq. (2.6) for τ an iterative solution must be used.

Table 2.4 presents the results of the calculated ultimate shear stresses obtained from Eq. (2.6) and compares these with the experimental average peak ultimate stress (τ_m) values. Included in the tabulation are the ultimate shear stresses (τ_c) calculated using the σ_{tcr} results of the square panel tests that correspond (same mortar, grout and constructed at the same time) to each set of double pier tests, as well as those τ_{ca} that correspond to the average σ_{tcr} value from all the square panel tests.

It is clear from Table 2.4 that, in general, this method overestimates the value of the ultimate shear stress given by the experimental test. The variations in the ratios $\frac{\tau_c}{\tau_m}$ and $\frac{\tau_{ca}}{\tau_m}$ reflect both the variation in the experimentally determined values of σ_{tcr} of the square panel results as well as the variation in the sets of double pier results. Seven of the eleven values of the ratio $\frac{\tau_{ca}}{\tau_m}$ which are based on the average value of all square panel tests, are within 25 percent of one. To obtain a better evaluation of this method, it is clear to the authors that better control over the mortar and grout strengths is necessary in future tests to eliminate this variation.

TABLE 2.1

EXPERIMENTAL STIFFNESS AND DISPLACEMENT VALUES OF HYSTERESIS ENVELOPES FOR THE SHEAR MODE OF FAILURE

Test No.	P_u Experimental (kips)	K_{e1} at 0.25 P_u [2] (kips/in)	K_{e2} at 0.9 P_u [2] (kips/in)	$\frac{K_{e1}}{K_o}$ [1]	$\frac{K_{e2}}{K_o}$ [1]	d_4/d_2 from Table 4.1 of Vol. 1	d_5 (in.)
1	26.0	430	270	0.93	0.58	1.55	0.59
2	33.2	490	270	1.06	0.58	1.55	0.53
3	27.3	410	180	0.88	0.39	1.50	0.77
4	26.0	440	130	0.95	0.28	1.80	0.83
5	20.5	420	200	0.91	0.43	1.55	0.65
6	25.5	440	210	0.95	0.45	1.85	0.71
7	40.7	510	210	1.10	0.45	1.50	0.70
8	48.4	520	130	1.12	0.28	1.45	0.85
9	29.5	545	420	1.17	0.91	2.10	0.64
10	34.1	575	410	1.24	0.88	2.80	0.51
11	20.0	435	260	1.11	0.66	3.80	0.56
12	21.8	410	270	1.04	0.69	5.10	0.65
17	23.7	410	170	0.88	0.37	1.60	0.50
				$\bar{x}$ = 0.99 without 9&10 $\bar{x}$ = 0.95	$\bar{x}$ = 0.50 without 9&10 $\bar{x}$ = 0.45	$\bar{x}$ = 2.16 without 11&12 $\bar{x}$ = 1.75	$\bar{x}$ = 0.65

NOTES:

(1) K_o = 464 kips/in. for fully grouted piers.

K_o = 392 kips/in. for partially grouted piers.

(2) The values of K_{e1} and K_{e2} are taken from Fig. 4.43 of Vol. 1[5].

TABLE 2.2

EXPERIMENTAL STIFFNESS AND DISPLACEMENT VALUES OF HYSTERESIS ENVELOPES FOR THE FLEXURAL MODE OF FAILURE

Test No.	P_{BC} Experimental (kips)	P_u Experimental (kips)	K_{e1} (1) (kips/in.)	K_{e2} (1) (kips/in.)	K_{e3} (1) (kips/in.)	$\frac{K_{e1}}{K_o}$	$\frac{K_{e2}}{K_o}$	$\frac{K_{e3}}{K_o}$	d_4/d_3	d_5 (in.)
13	20.4	29.1	205	120	75	0.44	0.26	0.16	1.8	1.0
14	19.3	28.8	230	125	105	0.50	0.27	0.23	3.1	0.9
15	20.5	35.2	230	130	70	0.50	0.28	0.15	2.5	1.5
16	21.8	36.2	240	160	65	0.52	0.35	0.14	3.4	1.3
						$\bar{x}$=0.49	$\bar{x}$=0.29	$\bar{x}$=0.17	$\bar{x}$=2.7	$\bar{x}$=1.2

NOTES:

(1) The values of K_{e1} and K_{e2} are taken from Fig. 4.43 of Vol. 1[5].

(2) K_o = 464 kips/in. for full grouted piers.

K_o = 392 kips/in. for partially grouted piers.

TABLE 2.3

COMPARISON OF THE MEASURED AND CALCULATED STRENGTHS FOR THE FLEXURAL MODE OF FAILURE

Test No.	A_s (in^2)	f_y (ksi)	f_u (ksi)	σ_c (psi)	N (kips)	P Experimental (kips)	P_y Calculated (kips)	P_u Calculated (kips)	$\frac{P}{P_y}$	$\frac{P}{P_u}$
3	0.39	54.1	83.4	125	24	27.3	30.5	40.4	0.90	0.68
4	0.39	54.1	83.4	125	24	26.0	30.5	40.4	0.85	0.64
7	0.88	78.1	108.8	250	48	40.7	84.0	108.0	0.48	0.38
8	0.88	78.1	108.8	250	48	48.4	84.0	108.0	0.58	0.45
13	0.39	50.8	74.9	125	24	29.1	29.3	37.5	0.99	0.78
14	0.39	51.7	76.5	125	24	28.8	29.6	38.1	0.97	0.76
15	0.39	51.8	73.9	125	24	35.2	29.7	37.2	1.19	0.95
16	0.39	51.3	75.7	125	24	36.2	29.5	37.8	1.23	0.96

TABLE 2.4

ULTIMATE SHEAR STRENGTH OF PIERS BASED ON THE CRITICAL TENSILE STRENGTH OF SQUARE PANELS

Test No.	Vertical Reinforcement	Horizontal Reinforcement	Applied Bearing Stress σ_c (psi)	Measured Ultimate Shear Stress τ_m (psi)	Square Panel Critical Tensile Stress σ_{tcr} (psi)	Calculated Ultimate Shear Stress Using σ_{tcr} τ_c (psi)	Calculated Ultimate Shear Stress Using Average σ_{tcr} (1) τ_{ca} (psi)	$\frac{\tau_c}{\tau_m}$	$\frac{\tau_{ca}}{\tau_m}$
1	2-#6	---	250	135	300	234	209	1.75	1.55
2	2-#6	---	250	173				1.35	1.21
3	2-#4	---	125	142	316	202	171	1.42	1.20
4	2-#4	---	125	135				1.50	1.27
5	2-#6	---	0	107	262	132	130	1.23	1.21
6	2-#6	---	0	133				1.00	0.98
7	2-#6	3-#5	250	212	306	235	209	1.11	0.99
8	2-#6	3-#5	250	252				0.93	0.83
9	2-#6	---	500	154	229	253	270	1.64	1.75
1C	2-#6	---	500	[illegible]				1.42	1.52
17	None	---	250	123	189	169	209	1.37	1.70

NOTE:

(1) The average critical tensile strength of all the square panels was 257 psi.

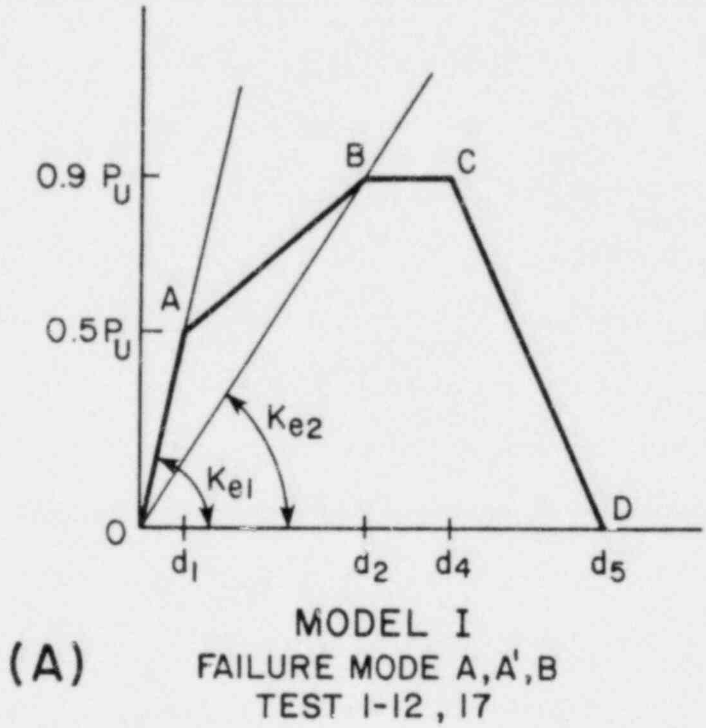

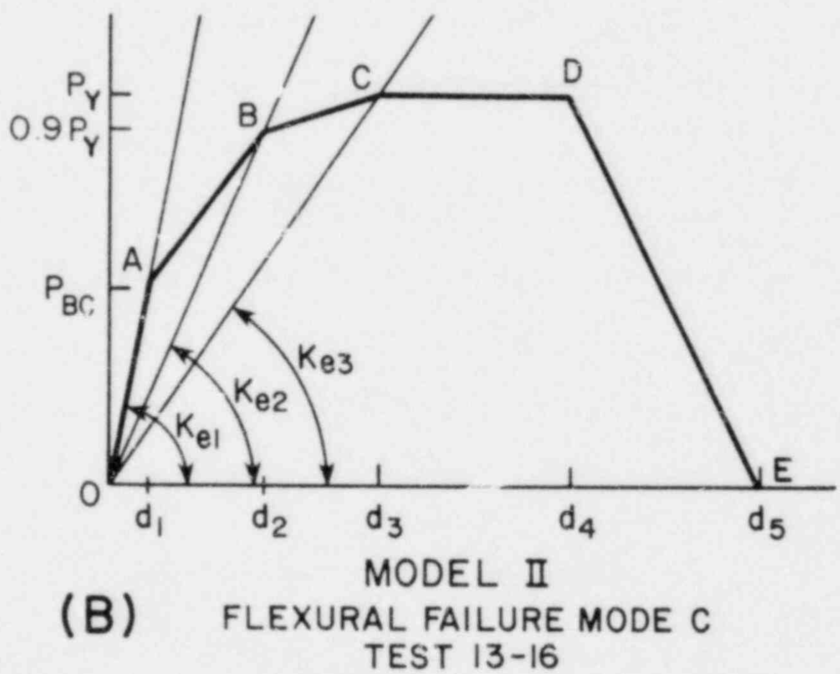

FIG. 2.1 IDEALIZED HYSTERESIS ENVELOPES

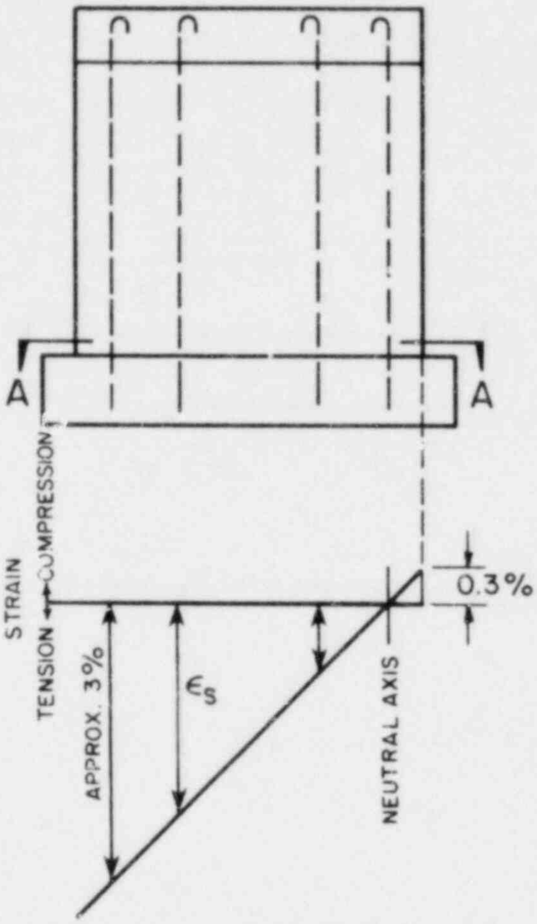

(a) STRAIN DISTRIBUTION AT AA

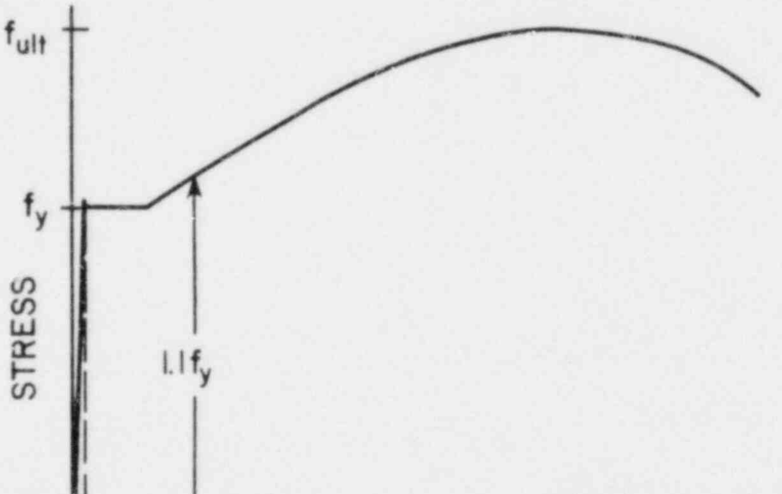

(b) STEEL STRESS-STRAIN CURVE

FIG. 2.2 STRAIN HARDENING ENHANCEMENT OF ULTIMATE LOAD

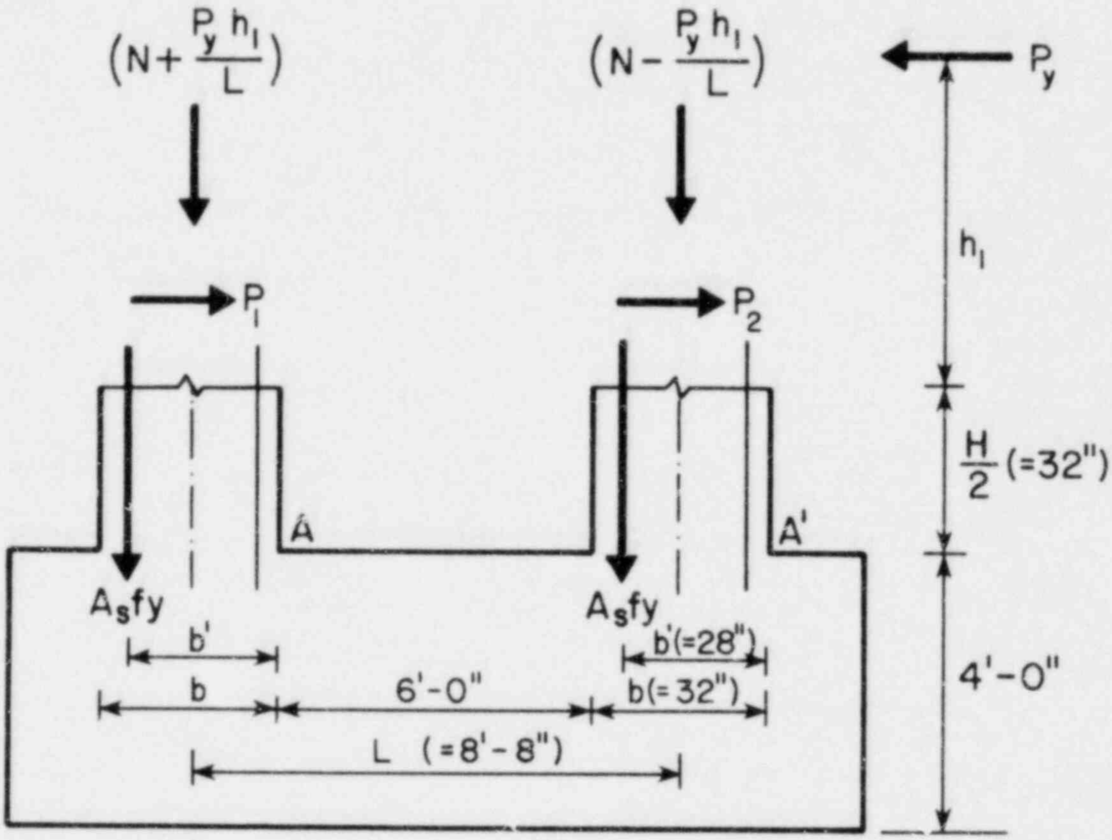

FIG. 2.3 ASSUMED FORCE DISTRIBUTION IN DOUBLE PIER

3. A COMPARISON OF DOUBLE PIER TEST RESULTS WITH OTHER INVESTIGATIONS

3.1 Introduction

Because of the relatively small amount of research that has been performed on the cyclic behavior of masonry structural elements, it is important to determine the consistency of the results obtained from the few test programs that have been carried out. This chapter therefore, presents a comparison of the results obtained in the double pier test program with results in the literature. Most of the results available prior to 1975 have been summarized in EERC Reports 75-15(7) and 75-21(28) and in Reference (29). As noted in these references, many different test techniques have been used in the studies performed to date, and many of the early test programs used monotonic shear loads. These factors are important when results from various tests programs are compared. The results for the effects of partial grouting, bearing stress, rate of loading, reinforcement and the inelastic characteristics of the structural behavior are compared in the following sections.

3.2 Effect of Partial Grouting

Four previous investigations have considered the effect of grouting on the shear strength of masonry elements. Of these, Moss and Scrivener(10) and Schneider(15) tested concrete block walls, whereas Blume(1) and Williams(16) tested clay brick walls. The results of the concrete block tests tend to confirm the results obtained in the present double pier test program in that for pseudo-static tests the net ultimate shear strength of the partially grouted walls is approximately equal to that of the fully grouted walls. The main difference in the behavior of the fully and partially grouted walls is in the rigidity of the walls. In Schneider's tests the partially grouted walls exhibited a considerable lack of rigidity in the lower load region, and in the region between first crack and ultimate load the increase in deflection was quite rapid with failure occurring rather suddenly.

In the double pier tests the ultimate net shear stress of the pseudo-static Tests 1 (full) and 11 (partial) are 135 and 132 psi, respectively. In the higher frequency (3 cps) Tests 2 (full) and 12 (partial) the corresponding stresses are 173 and 143 psi, respectively. It therefore appears that the higher frequency test increases the strength of the fully grouted pier since the net stresses of Tests 1, 11 and 12 are approximately the same. Furthermore, the stiffness degradation of the partially grouted walls observed by Schneider was not nearly as substantial in the double pier tests (see Figs. 4.38, 4.42 and 4.43 of Volume 1[5]).

The results obtained by Blume [1] and Williams [16] for clay brick walls are conflicting. Blume, using the test setup shown in Fig. 1.1, concluded that fully grouted clay brick walls had a substantially greater ultimate net shear strength than partially grouted walls. The one comparative test that Williams performed with a cantilever test setup produced approximately equal net shear stresses for the fully and partially grouted walls. Because of the very different test techniques used in these two test programs no conclusions can be drawn yet, and the effect of partial grouting on clay brick walls will be investigated further in the single pier test program.

3.3 Effect of Bearing Stress

The bearing load has been found to be an important parameter in determining the shear strength of a masonry element in all investigations that have considered it. In all cases the shear strength was found to increase with an increase in the bearing load. In addition to its effects on the strength of an element, the bearing load also affects the mode of failure and post-elastic behavior of walls.

Both Meli[17] and Williams[16] showed that identical walls with bearing stresses of 125, 250 and 500 psi demonstrated flexural, transitional and shear modes of failure, respectively. Their results indicate that the ultimate strength increases and the ductility decreases as a result of the different modes of failure; this behavior implies a beneficial effect in the elastic region and a detrimental effect in the inelastic region.

In both the double pier tests and in Priestley and Bridgeman's tests[18], the effect of the bearing load on the shear mode of failure was investigated and the conclusions from both these studies are that an increase in bearing load both increases the ultimate shear strength and improves the inelastic behavior. Figures 4.37, 5.2 and 5.3 of Volume 1[5] graphically illustrate this conclusion for the double piers with bearing stresses of 0,250 and 500 psi.

Williams and Meli did not thoroughly investigate the effect of bearing load on the shear mode of failure and their generalization on the effect of bearing load is not validated by either Priestley and Bridgeman's results or the double pier test results. Clearly, because of the importance of the bearing load on the behavior of piers and the conflicting conclusions at present available, additional test data are required on the effect of this important parameter.

3.4 Effect of Rate of Loading

Williams[16] was the first to compare the effects of dynamic and pseudo-static cyclic load tests on masonry piers. His four comparative tests were performed with test frequencies below 1 cps. Three of the four walls that he tested failed in shear and indicated similar results in both the pseudo-static and dynamic tests. For the one wall that failed in the flexural mode, the dynamic test showed less desirable inelastic behavior than the pseudo-static test. This led Williams to conclude, contrary to the normally accepted opinion,that cyclic pseudo-static test data may be inappropriate for use as a conservative basis for the seismic design of reinforced masonry buildings.

The double pier tests did not support Williams'conclusion. For the walls that failed in the shear mode the ultimate strength of the pseudo-static tests ranged from as much as 23 percent less than to approximately equal to the corresponding dynamic (3 cps) test result. Moreover, the shapes of the hysteresis envelopes (Figs. 4.37 to 4.40 of Volume 1) for the pseudo-static tests were less favorable than for the corresponding dynamic tests. Hence, for the shear mode of failure the double pier investigation indicates that the pseudo-static cyclic tests do produce conservative results when compared to dynamic tests.

For the walls that failed in the flexural mode in the double pier tests (Tests 13 to 16) there was little or no difference between either the strength or the shape of the hysteresis envelopes for the corresponding pseudo-static and dynamic loadings. This behavior is in contrast with results reported from Williams' one test on a cantilever test specimen; therefore, the results of the double pier tests can be interpreted to give the opposite conclusion to that stated by Williams, demonstrating that additional test data are required on this variable.

3.5 Effect of Reinforcement

The effect of reinforcement on the shear strength of a masonry element has to be considered in conjunction with the mode of failure. Until the paper presented by Priestley and Bridgeman[18] in 1974, it was widely believed that horizontal and vertical reinforcement were equally effective in developing the full shear strength of masonry, and that only 0.3 percent bd reinforcement (where b is the width and d the thickness of the wall) was required to achieve this. These conclusions were based mainly on the investigations of Schneider [13,15] and Scrivener[10]. Priestley and Bridgeman's results disagreed with both of these conclusions. They demonstrated that horizontal steel is approximately three times as efficient as vertical steel in carrying the shear force across a diagonal crack and that a larger quantity than 0.3 percent bd of shear steel is effective in improving the ultimate shear capacity of masonry.

Priestley et al.[18,27] have performed several extensive series of tests on cantilever piers and have shown that very desirable inelastic behavior can be obtained with the flexural mode of failure. For cantilever piers, it is necessary to provide sufficient shear strength by means of horizontal reinforcement to exceed the flexural strength, using a capacity design approach. Priestley has recommended that the total area of shear steel crossing a potential 45° shear crack in a pier be calculated as follows:

$$V_D = \frac{\phi_o}{\phi_f} V_B \tag{3.1}$$

where V_B is the shear force required to induce yielding of all the vertical steel in the pier, ϕ_f is the flexural undercapacity factor (recommended as 0.7 for masonry design), and ϕ_o is the flexural overcapacity factor representing the ratio of maximum feasible flexural strength to ideal flexural strength based on nominal material strengths (recommended as 1.25 for 40 ksi steel and 1.4 for 60 ksi steel). V_D is the shear force used to calculate the required area of horizontal steel, A_{hs}, as follows:

$$A_{hs} = \frac{V_D}{\phi_s f_y} \tag{3.2}$$

where ϕ_s is the shear capacity reduction factor (recommended as 0.85) and f_y is the yield stress of the horizontal steel.

There are two major problems associated with this design procedure. One is sliding shear along the base of the pier or wall when a flexural mode of failure is forced to occur. This was evident in Priestley's tests and led to a limitation of the design shear force in his recommended design method. The second problem is the inherent assumption that a wall can develop the shear capacity of the horizontal steel, $A_{hs}f_y$. This assumption was not validated in the double pier tests, and is discussed in Section 3.5.2 below.

3.5.1 Effect of Reinforcement in the Flexural Mode of Failure

Several investigators have shown that the ultimate strength in the flexural mode of failure can be determined with reasonable accuracy by applying the basic concepts developed for reinforced concrete; this idea is discussed in detail in Section 2.3.1. Meli(17), Williams(16) and Priestley and Bridgeman(18,27) have all stated that the flexural mode of failure is characterized by a secondary compressive failure at the toe of the wall. Such a failure is caused by the decrease in the area of masonry under compression as the steel yield strain increases (Fig. 2.2) finally resulting in compressive stresses that exceed ultimate. This causes splitting and spalling of the masonry with a resultant loss in confinement and eventual buckling of the vertical steel. Severe load degradation and ultimate failure of the wall follow.

Priestley and Bridgeman also performed a series of tests using a joint reinforcement plate similar to the 1/8 in. plate used in Tests 15 and 16 (shown in Fig. 2.4 of Volume 1). They found that the plate alleviated much of the splitting and spalling associated with the secondary compressive failure, leading to improvement in the inelastic behavior. This improvement was also observed in the present double pier tests and is graphically shown in Fig. 4.40 of Volume 1, where results for Tests 13 to 16 are compared. Priestley and Bridgeman concluded that if the 1/8 in. plate is not present the yield strength of the vertical reinforcement should be used to calculate the ultimate capacity of the walls, but if joint reinforcement is present then the ultimate strength of the vertical reinforcement should be used. This conclusion is also supported by the double pier tests, as seen in Table 2.3, where the calculated and measured ultimate flexural strengths are compared for tests with and without the joint reinforcement (Tests 13 to 16).

In summary, the flexural mode of failure is governed by the capability of a wall to develop shear loads exceeding its computed flexural capacity. The flexural capacity of the wall is governed by its width, vertical load and amount of vertical reinforcement. The shear capacity of a wall is discussed in the following section.

3.5.2 Effect of Reinforcement in the Shear Mode of Failure

When failure is in the shear mode, Schneider(13) and Scrivener et al.(10) concluded that a quantity of horizontal and vertical shear reinforcement equal to 0.3 percent bd (where b is the width and d the thickness of the element) is sufficient to develop the shear strength of the wall or pier. Schneider(13) concluded in the case of concrete block walls, that little difference existed between the ultimate loads sustained by similarly constructed walls reinforced on the basis of 0.3 percent bd and 0.2 percent bd; hence, 0.2 percent bd was presumed sufficient to develop the ultimate shear resistance of the grouted masonry. He also stated that the load at which the first crack was formed was noticeably lowered by a reduction in the amount of reinforcement. Scrivener[10] concluded that vertical and horizontal reinforcement are equally effective in providing satisfactory crack behavior and failure loads. Walls with evenly distributed reinforcement exhibit a later onset of severe cracking than walls where the reinforcement is concentrated in the periphery. With a low percentage of reinforcement, failure occurs soon after the onset of severe cracking. With higher percentages of reinforcement, the failure load is much greater than the load causing severe cracking. Higher failure loads were obtained for walls with higher percentages of reinforcement up to 0.3 percent of the gross cross-sectional area. Above this percentage, reinforcement had little effect on the failure load.

In contrast, Priestley and Bridgeman[18,27] demonstrated that horizontal steel is approximately three times as efficient as vertical steel in carrying shear force across a diagonal crack, and that a larger quantity than 0.3 percent bd of shear steel is effective in improving the ultimate shear capacity of masonry. For this larger quantity of shear reinforcement to be effective, they stated that the quantity (preferably horizontal) should be sufficient to resist the full ultimate flexural lateral load, so that a flexural mode of failure is induced.

Table 3.1 summarizes the results of various tests and presents a comparison of the increase in shear strength with the increase in the amount of horizontal reinforcement. It is clear that the increase in ultimate strength does not correlate with the increase in the quantity of reinforcement. Furthermore, the shear capacity of Tests 7 and 8 in the double pier tests should have developed close to the $A_{hs}f_y$

capacity of the horizontal reinforcement according to Priestley's design method. This was not the case, and because of this discrepancy and the lack of consistency of other test results, the effect of horizontal reinforcement in the shear mode of failure will be studied extensively in the single pier test program. Until these or other extensive test results are available to resolve the discrepancies, Priestley's suggested design method should be used with extreme caution.

3.6 Inelastic Characteristics

Determination of the inelastic characteristics of a structural element is the objective of most experimental earthquake related studies. The inelastic behavior is generally defined as the behavior after the yield and/or ultimate load of a structural element has been attained. From a structural design viewpoint the inelastic behavior is extremely important because many buildings are designed to withstand moderate earthquakes without reaching the yield or ultimate strength of the structural elements, but are expected to be damaged during intense earthquakes.

In evaluating the inelastic characteristics of a pier, hysteresis envelopes (Figs. 4.37 to 4.40 of Volume 1) provide a good qualitative picture; however, they must be considered in conjunction with other parameters to evaluate fully the inelastic behavior. The other parameters include the energy dissipated per cycle, the ultimate strength, indicators of ductility, and comparisons of crack patterns at equal displacements. The main advantage of hysteresis envelopes is that they provide visual comparisons of ductility and ultimate strength; however, they give no indication of the energy dissipated per cycle.

The question to be considered is what constitutes desirable inelastic behavior. It is difficult to answer this question in quantitative terms, but Figs. 3.1a, b, and c are useful for a qualitative discussion of three different aspects of the behavior. Figure 3.1a shows a set of four force-deflection relationships, each with the same ultimate strength (F_1). Obviously, the inelastic force-deflection relationship becomes more favorable in passing from curves A through D. Figure 3.1b shows a set of four force-deflection relationships with different ultimate strengths. The relative merit of these curves is more difficult to evaluate, as it is a function of the imposed interstory deflection. If the interstory deflection never exceeds d_1, then piers with the force-deflection relationships given by B, C and A are preferable to those of D. If the interstory deflection increases to d_2, then B, C and D are preferable to A; and finally, if the interstory deflection increases to d_3, then the order of increasing preference is A, B, C and D. Hence, the relative merit of the force-deflection relationships in Fig. 3.1b depends on the intensity of the expected earthquake. For a moderate earthquake where the interstory deflection may not exceed d_1, the order of increasing preference would be D, C, A and B. If, however, a large earthquake is considered, and the interstory deflection could be of the order of d_3, the order of increasing preference would be A, B, C and D. (It should be noted that the interstory deflection resulting from a particular earthquake is a function of the dynamic characteristics of the building as well as the earthquake). For the two force-deflection relationships given by Fig. 3.1c, obviously B is preferable to A, as it is able to resist a greater lateral force and has the same characteristics when the interstory deflection exceeds d_1.

With the foregoing discussion in mind the inelastic characteristics of walls tested in various investigations will be compared in the following two sections. The first section deals with load degradation of the piers while the second will discuss ductility indicators used in various test programs.

3.6.1 Load Degradation

Load degradation, or strength deterioration, in the context of this report is the drop in load carrying capacity of a particular element between successive cycles of loading at the same amplitude. It is discussed in conjunction with mode of failure in the following subsections.

(a) Load Degradation Associated with the Flexural Mode of Failure.

Meli[17], Williams[16] and Priestley and Bridgeman[18,27] all observed similar features of load degradation associated with the flexural mode of failure. Meli found that concrete block walls whose failure was governed by flexure showed little deterioration before yielding of the reinforcement. After yielding, significant reduction of stiffness occurred in subsequent cycles but strength was not affected. For high deformations (large displacements) progressive crushing of the unconfined compression corner gave rise to major deterioration of the load carrying capacity.

For cantilever walls failing in flexure, Williams observed very similar behavior. For several cycles at constant amplitude the major deterioration was between the first and second cycles; additional cycles at the same amplitude were relatively stable. He also observed that for large displacements, the unconfined corner was subjected to progressive crushing which finally led to a sudden deterioration in the load carrying capacity.

Priestley and Bridgeman found that for all walls failing in flexure, sudden load degradation occurred after initial loading to displacements corresponding to ductilities of the order of 5. At these displacements vertical cracks developed close to the toe and the resulting isolated columns of brick work were "blown out" under the combined action of shear and compression. This resulted in loss of bond for the extreme tension bars on reversal of the load direction, compounding the effect. Furthermore, after initial load reversals any steel close to such a crushing zone became inadequately supported laterally and buckled. Degradation rapidly increased as this process continued with each load reversal.

In order to suppress the undesirable load degradation associated with the flexural failure mechanism, Priestley and Bridgeman inserted 1/8 in. plates in the mortar joints in the vicinity of the compressive toes of the wall and tested five walls with the joint plates inserted. They concluded from these tests that all five walls showed an ability to sustain several cycles of loading at ductility factors of 4 or more with peak loads remaining above or close to the yield load.

For the double pier tests without mortar joint plates (Tests 13 and 14), the behavior was similar to that noted by others. There was no load degradation in successive cycles at the same amplitude before yielding of the vertical reinforcement; however, after yield there was some small load degradation between the first and second cycles with additional cycles being relatively stable.

The double piers with the mortar joint plates (Tests 15 and 16) showed an excellent post-elastic behavior with the ability to sustain several cycles of loading at large displacements and with peak loads remaining above or close to the average ultimate strength.

(b) Load Degradation Associated with the Shear Mode of Failure.

Meli[17] observed that for walls with interior reinforcement whose failure was governed by shear, very significant strength deterioration occurred after the formation of diagonal cracks. Often the load-deflection curve did not stabilize, and initial strength could not be attained again. Increasing the amount of interior reinforcement did not markedly improve this behavior.

Williams[16] found that walls failing predominantly in shear developed large initial stiffness degradation with severe load degradation, after diagonal cracking had occurred and that further degradation occurred at each subsequent cycle. Priestley and Bridgeman[18,27] found that cantilever walls failing in shear exhibited rapid degradation of load on successive load reversals after major diagonal cracking.

Test results presented in Figs. 4.1 to 4.12 of Volume 1 did not, in all cases, show such a rapid load degradation as that observed by the previous investigators. However, this difference in most cases is attributable to the different load sequences used in the various investigations. For each of the three cycles of loading at the same amplitude there was some load degradation, and this became more substantial after the ultimate load was attained. The piers with a lower bearing load showed less rapid load degradation after the ultimate load was attained, (compare Tests 5 and 6 with Tests 1 and 2, and with Tests 9 and 10 in Figs. 4.1, 4.2, 4.5, 4.6, 4.9 and 4.10 of Volume 1). The piers with partial grouting (Tests 11 and 12) had less load degradation than the piers with full grouting (Tests 1 and 2), (see Figs. 4.1, 4.2, 4.11 and 4.12 of Volume 1).

The load degradation characteristics of a wall after major cracking has occurred are important variables to be used in calculating its inelastic characteristics. It is clear that for the shear mode of failure the post-cracking behavior is not nearly as favorable as the post-yield behavior in the flexural mode of failure.

3.6.2 Ductility

Ductility is a term that is used in earthquake related experimental studies to provide an indication of the inelastic performance of structural elements. Generally for steel and reinforced concrete structural elements, the ductility ratio provides a reasonable comparable measure of the inelastic performance for the elements. The generally accepted definition of ductility ratio is the ratio of the maximum displacement (or rotation) at which the ultimate or yield load can no longer be maintained to the displacement (or rotation) at which the yield load is first attained. For masonry structural elements the ductility ratio concept must be used with caution. For instance, Tests 1 and 8 of the double pier tests have the same values of ductility indicators

$$\frac{\delta_1 + \delta_2}{2} \quad \text{and} \quad \frac{\delta_3 + \delta_4}{2}$$

(defined in Section 4.3 and given in Table 4.1 of Volume 1), but from the hysteresis envelopes shown in Fig. 4.39 of Volume 1, Test 8 obviously has a much more desirable inelastic behavior.

From the results presented in the state of the art report[28] it is clear that both the ductility and the inelastic characteristics are significantly affected by the test technique, the mode of failure, the quantity and distribution of reinforcement and the nature of loading (monotonic or cyclic). The ductility of walls will be discussed with respect to the modes of failure in the following two subsections.

(a) Ductility in the Flexural Mode of Failure.

The force-deflection relationships of the cantilever walls tested cyclically by Williams [16] exhibited ductility ratios at the ultimate load of between 2 and 4. The loss of load-carrying capacity was attributed to the secondary compressive failure at the toes of the walls.

In the monotonic tests performed by Meli[17], substantial ductile capacity was observed for the flexural mode of failure. Based on Meli's definition of ductility, walls failing in flexure had ductility ratios exceeding four. Although he did not define or quantify ductility ratios for the cyclic tests he performed, he stated that the behavior of walls with interior reinforcement whose failure is governed by flexure is nearly elasto-plastic with remarkable ductility.

Priestley and Bridgeman[18,27] stated that load degradation following flexural failure occurred after loading to displacement ductilities of the order of 5. Because complete load-deflection time histories are not presented for these tests it is difficult to determine how the results compare with those of Williams and Meli. However, Priestley and Bridgeman did attribute the sudden drop in load-carrying capacity to the secondary compression failure. Walls containing the 1/8 in. plate in the mortar joints at the compressive toes were observed to have ductilities of at least 5 and sometimes as high as 16 at the yield load. The hollow unit walls were also adequately confined for ductility ratios up to 5.

The definition of ductility indicators used in the double pier tests produces slightly lower values than those noted by other investigators. The ductility indicators for Tests 13 and 14 at the average ultimate load (90 percent of peak ultimate load) are 1.8 and 3.1, respectively, and 5.2 and 6.6 at the working ultimate load (70 percent of peak ultimate load), respectively. These ratios were improved with the introduction of the plates in the mortar joints of Tests 15 and 16. Then the values at the average ultimate load are 2.5 and 3.5, respectively, and 9.2 and 10.5, respectively, at the working ultimate load.

Although there is variation in the values of the ductility indicators for the flexural modes of failure of the various investigations, most values lie between 2 and 4 and these are significantly improved with the introduction of the 1/8 in. steel plate in the mortar joint.

(b) Ductility in the Shear Mode of Failure.

For the tests performed by Williams[16], the ductility ratios of the cantilever walls tested cyclically and failing in shear varied between 1 and 2. It is difficult to compare the ratios of the different tests, because each wall was subjected to a different displacement history. However, it is apparent from the results presented that the walls were not able to maintain the ultimate load over a very large displacement range.

For the monotonic tests performed by Meli[17], his ductility ratios for the shear mode of failure exceeded 1.75. He also stated that if failure is governed by diagonal cracking, ductility is less than in the flexural mode of failure and when vertical loads are applied the behavior is quite brittle.

Although Priestley and Bridgeman[18] did not mention the ductility of walls failing in shear, they stated that for walls without bearing load, failure occurred soon after the formation of the diagonal crack with large horizontal displacements across the diagonal crack associated with severe load degradation, and hence a ductility ratio close to 1. For walls with an applied bearing load, the degradation was not as severe although no mention was made of the ductility capacity.

For the fully grouted double piers with bearing stresses less than 250 psi, the ductility indicators at the average ultimate load ranged from 1.45 to 1.8, and these values are consistent with those observed by Meli and Williams. As the bearing load increased to 500 psi in Tests 9 and 10, the corresponding ductility indicators were 2.1 and 2.8, respectively. This improvement in inelastic behavior is consistent with that observed by Priestley.

For the partially grouted double piers (Tests 11 and 12) the ductility indicators at the average ultimate load were 3.8 and 5.1, a significant increase over the fully grouted piers. However, if the overall inelastic performance of the piers is evaluated from the hysteresis envelopes (Fig. 4.38 of Volume 1) the increase in the ductility ratio does not reflect an improvement in the inelastic characteristics when compared to Test 12. This anomaly was discussed in the introduction to this section.

For the shear mode of failure it is clear that the ductility ratios are less than those of the flexural mode of failure, and most test values lie between 1 and 2.

TABLE 3.1

THE EFFECT OF INCREASED REINFORCEMENT ON THE SHEAR STRENGTH

Author And Reference No. of the Investigation	Reference Code Used in the Paper	Reinforcement of the Walls			Ultimate Strength (kips)	Increase in Reinforcement		Increase in Strength (kips)
		Horizontal	Vertical Interior	Vertical Periphery		Horizontal $(A_s f_y)^{(3)}$	Vertical	
Scrivener (9)	C9	---	2 - 1/2"	2 - 5/8"	60.0	---	1 - 1/2"	10.0
	C3	---	3 - 1/2"	2 - 5/8"	70.0			
	C3	---	3 - 1/2"	2 - 5/8"	70.0	2 - 1/2" (15.7)	---	34.0
	D12	2 - 1/2"	3 - 1/2"	2 - 5/8"	104.0			
	D13	3 - 5/8"	3 - 5/8"	2 - 5/8"	96.0	1 - 5/8" (12.3)	---	14.0
	D14	4 - 5/8"	3 - 5/8"	2 - 5/8"	112.0			
Williams (16)	A1	---	---	2 - 7/8"	37.5	2 - 5/8" (24.5)	---	2.5
	A2	2 - 5/8"	---	2 - 7/8"	40.0			
Mayes & Clough (19)	1(1)	---	---	4 - 3/4"	26.0	3 - 5/8" (62.4)	---	14.7
	7(1)	3 - 5/8"	---	4 - 3/4"	40.7			
	2(2)	---	---	4 - 3/4"	34.3	3 - 5/8" (62.4)	---	12.5
	8(2)	3 - 5/8"	---	4 - 3/4"	46.8			
Prestley & Bridgeman (18)	F7	---	6 - 3/4"	2 - 3/4"	62.1	2 - 1/2" (23.6)	---	2.9
	F8	3 - 1/2"	6 - 3/4"	2 - 3/4"	65.0			

(1) Tests performed pseudo-statically.

(2) Tests performed at a frequency of 3 cps.

(3) f_y is assumed to be 40 ksi, except for the double pier tests where the actual value is used and $A_s f_y$ is expressed in kips.

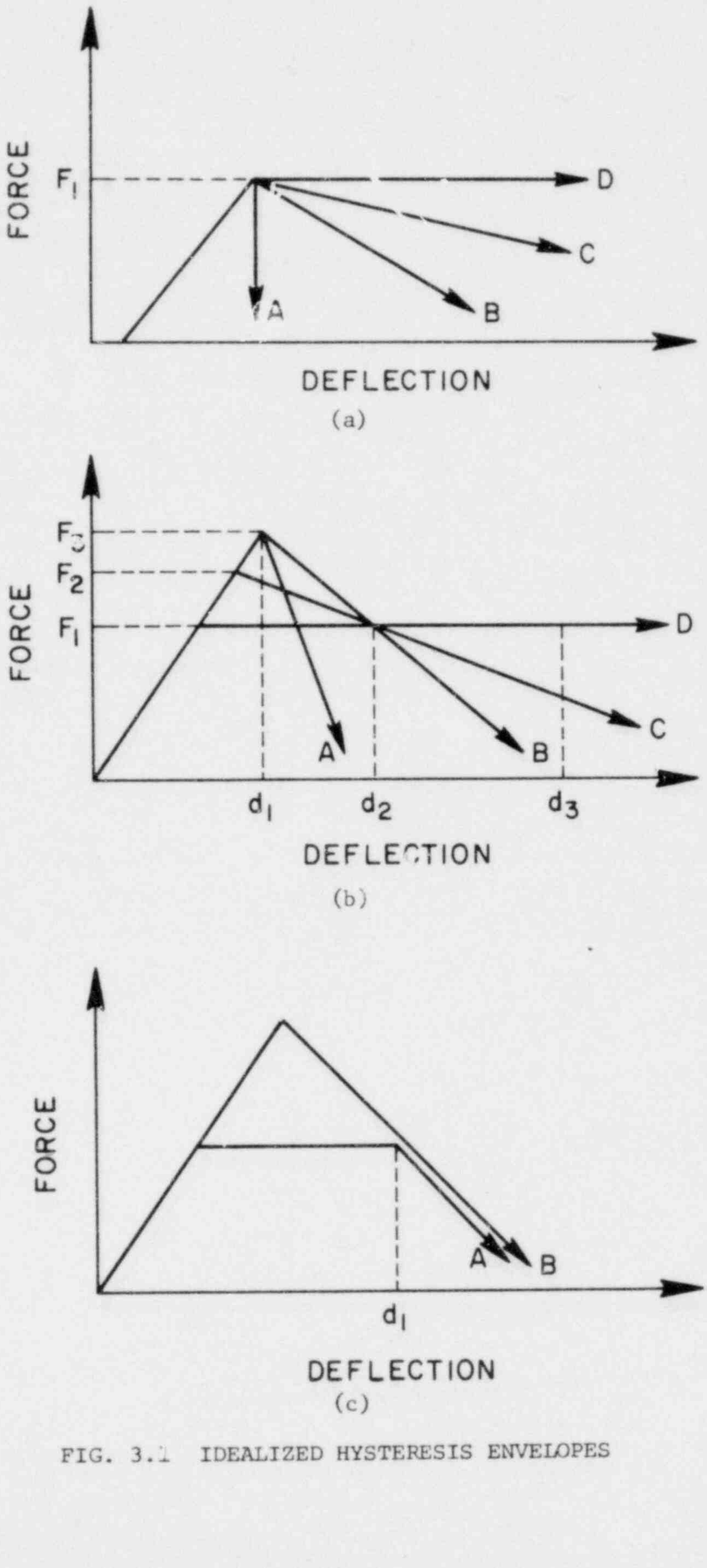

FIG. 3.1 IDEALIZED HYSTERESIS ENVELOPES

4. SUMMARY

The preceding three chapters have provided an analysis of the test results presented in Volume 1[5]. The first chapter presents a comparison of the critical tensile strengths obtained from the double pier tests with those obtained from a simple diagonal compression test on a square panel. The objective of these tests was to evaluate an alternative simplified method of determining the shear strength of masonry walls. Currently, code values are based on f'_m, the compressive strength of a prism test. The authors are encouraged by the comparison of the average values of the critical tensile strengths obtained from the double pier and simplified tests; at the same time, however, they are disturbed by the wide scatter of the results. Part of the scatter can be attributed to the acknowledged lack of control over the mortar and grout strengths used in the test specimens. This variation was permitted because the authors wanted to include workmanship as a parameter in the test program. However, it is clear that better control over the mortar and grout strengths will be required in future tests to obtain satisfactory correlation.

Chapter 2 of the report presents theoretical models of the hysteresis envelopes obtained in the double pier tests. The ultimate objective of formulating these models is to provide a basis for performing an inelastic response analysis of multistory masonry buildings subjected to earthquake ground motions. The approach being followed is similar to that used for reinforced concrete and steel buildings; the inelastic behavior of typical structural components is determined experimentally and idealized inelastic models are then developed which adequately describe the behavior of the components. The models at a later date will be incorporated into an inelastic analysis computer program which deals with the entire building.

Parameters included in the models define stiffness and ductility exhibited at various stages of the hysteresis envelopes as well as the ultimate and/or yield strengths of the piers. The stiffness and ductility parameters were determined from average values of the experimental results, whereas the ultimate and/or yield strengths were obtained from theoretical formulations and then compared with the experimental results.

The variation in the stiffness and ductility parameters determined for the proposed model in the shear mode of failure was significant, and before this model is used in a computer program to determine the overall response of a building to an earthquake ground motion, a sensitivity study should be performed to determine what effect the range of each variable has on the overall response of the building. The same parameters had much less variation for the flexural mode of failure, and a model based on these average values should be reasonably accurate.

The formulation presented in Chapter 2 for determining the yield and ultimate strength in the flexural mode of failure was similar to that previously used by others and it produced good agreement with the experimental results. The formulation for determining the ultimate strength in the shear mode of failure generally overestimates the experimentally determined values. Seven of the eleven computed values were within ± 25 percent of the experimental values; however, the other four covered a much larger range.

It should be noted that the hysteresis models presented in Chapter 2 are for piers with a height to width ratio of two, and until additional tests are performed with other aspect ratios the models can be considered valid only for this geometry. Furthermore, the hysteresis envelopes are idealized from a displacement controlled test with gradually increasing magnitude; therefore, these results should be validated later with loading more random in nature.

Chapter 3 presents a comparison of the double pier test results with those obtained by other investigators. Because there has been a relatively small amount of research on the cyclic behavior of masonry structural elements, the authors felt it was important to determine the consistency of the results obtained in the few test programs that have been performed. The comparisons are presented in terms of the effects of partial grouting, bearing stress, rate of loading, reinforcement and inelastic characteristics.

The three investigations that considered the effect of partial grouting on hollow concrete block walls all reached the conclusion that the net ultimate strength of fully and partially grouted walls is approximately equal. The two investigations that considered the effect of partial grouting on hollow clay brick walls came to contradictory conclusions. Therefore, this variable will be studied further in the EERC eighty single pier test program.

The bearing load was found to be an important parameter in all investigations that included it as a variable. It has an important effect in controlling the mode of failure of a wall: the greater the bearing load, generally, the greater the likelihood of a shear failure. With respect to its effect on the inelastic characteristics in the shear mode of failure, two studies found that increased bearing load improved the inelastic behavior. However, this observation conflicted with the generalized conclusion of the two other investigators. Clearly additional test data are required on the effect of this important parameter.

The effect of the rate of loading on the shear mode of failure was included in two studies and both found that the pseudo-static cyclic tests produce conservative results when compared to dynamic tests. For the flexural mode of failure, conflicting results were obtained from the two studies that included this as a parameter. One study found that the pseudo-static tests produced non-conservative results while the double pier tests indicated there was little difference between the pseudo-static and dynamic tests.

The effect of horizontal reinforcement on the ultimate strength in the shear mode of failure appears to be the least consistent result. It is clear that there is little correlation between the ultimate strength and the amount of horizontal reinforcement. However, one study concludes that the shear mode of failure can be suppressed with a sufficient amount of horizontal reinforcement and a proposed design method is based on this premise. This effect was not extensively studied in the double pier tests, but will have a high priority in the single pier test program.

The inelastic characteristics of walls are discussed in terms of ductility and load degradation. For the shear mode of failure, the ductility of the walls was found to be between 1 and 2 in most test programs. Load degradation was generally severe for this mode of failure after the initial diagonal crack developed. The severity of the load degradation was found to reduce as the bearing load increased. For the flexural mode of failure the ductility of the walls was found to be between 2 and 4 in most test programs and load degradation was not severe until the maximum ductility had been attained. The load degradation then was attributed to the secondary compressive failure at the toes of piers. The introduction of 1/8 in. plates in the mortar joints at the toes of a wall significantly increased the ductility and generally prevented the severe load degradation associated with the secondary compressive failure.

Significant progress has been made in the last decade on understanding the inelastic behavior of masonry walls. However, much remains to be done before researchers and structural designers can predict, within reasonable bounds, the response of a multistory masonry building to earthquake ground motions.

REFERENCES

1. Blume, J. A. and Proulx, J., "Shear in Grouted Brick Masonry Wall Elements," Western States Clay Products Association, San Francisco, California, Copyright 1968.

2. Borchelt, J. G., "Analysis of Brick Walls Subject to Axial Compression and In-Plane Shear", Proceedings of Second International Brick Masonry Conference, Stoke-on-Trent, April 1970.

3. Degenkolb, H. J. and Associates, "Bed-Joint Shear Tests of Cylindrical Cores Compared with Diagonal Compression Tests of Brick Masonry Wallettes", Testing Engineers Incorporated, March 1975.

4. Yokel, F. Y., and Fattal, S. G., "Ultimate Load Capacity of Masonry Bearing Walls", ASCE National Conference, New Orleans, April 1975.

5. Mayes, R. L., Omote, Y. and Clough, R. W., "Cyclic Shear Tests of Masonry Piers, Vol. I - Test Results", EERC Report No. 76-8, University of California, Berkeley, May 1976.

6. Frocht, M. M., "Recent Advances in Photoelasticity", Transactions ASME, Vol. 55, AER-WDI, pp. 135-153, 1931.

7. Mayes, R. L. and Clough, R. W., "A Literature Survey - Compressive, Tensile, Bond and Shear Strength of Masonry", EERC Report No. 75-15, University of California, Berkeley, July 1975.

8. Schneider, R. R., "Tests on Reinforced Grouted Brick Masonry Shear Panels", Report issued by California State Division of Architecture, Los Angeles, 1956.

9. Scrivener, J. C., "Static Racking Tests on Masonry Walls", Designing, Engineering and Constructing with Masonry Products, Edited by F. B. Johnson, Gulf Publishing Co., Houston, Texas, May 1969.

10. Moss, P. J. and Scrivener, J. C., "Concrete Masonry Wall Panel Tests - The Effect of Cavity Filling on Shear Behaviour", New Zealand Concrete Construction, April 1968.

11. Structural Clay Products Research Foundation, "Compressive, Transverse and Racking Tests of 4" Brick Walls", SCPRF, Research Report No. 9, 1965.

12. Structural Clay Products Research Foundation, "Compressive, Transverse and Racking Strength Tests of Four Inch Structural Clay Facing Tile Walls", SCPRF, Research Report No. 11, 1967.

13. Schneider, R. R., "Lateral Load Tests on Reinforced Grouted Masonry Shear Walls", University of Southern California Engineering Center, Report No. 70-101, 1959.

14. Scrivener, J. C., "Concrete Masonry Wall Panel Tests - Static Racking Tests with Predominant Flexural Effect", New Zealand Concrete Construction, July 1966.

15. Schneider, R. R., "Shear Tests in Concrete Masonry Piers", Report of California State Polytechnic College, Pomona, California.

16. Williams, D., "Seismic Behaviour of Reinforced Masonry Shear Walls", Ph.D. Thesis, University of Canterbury, New Zealand, 1971.

17. Meli, R., "Behaviour of Masonry Walls Under Lateral Loads", Proceedings of Fifth World Conference on Earthquake Engineering, Rome, 1972.

18. Priestley, M. J. N., and Bridgeman, D. O., "Seismic Resistance of Brick Masonry Walls", Bulletin of the New Zealand National Society for Earthquake Engineering, Vol. 7, No. 4, December 1974.

19. Mayes, R. L., and Clough, R. W., "Cyclic Tests on Concrete Masonry Piers", 44th Annual Convention of Structural Engineers Association of California, San Diego, October 1975.

20. Greenley, D. G., and Cattaneo, L.E., "The Effect of Edge Load on the Racking Strength of Clay Masonry", Proceedings of Second International Brick Masonry Conference, Stoke-on-Trent, April 1970.

21. Haller, P., "Load Capacity of Brick Masonry", Designing, Engineering and Constructing with Masonry Products, Edited by F. B. Johnson, Gulf Publishing Co., Houston, Texas, May 1969.

22. Turnsek, V., and Cacovic, F., "Some Experimental Results on the Strength of Brick Masonry Walls", Proceedings of Second International Brick Masonry Conference, Stoke-on-Trent, April 1970.

23. Pieper, K., and Trautsch, W., "Shear Tests on Walls", Proceedings of Second International Brick Masonry Conference, Stoke-on-Trent, April 1970.

24. Sinha, B. P., and Hendry, A. W., "Racking Tests on Storey Height Shear-Wall Structures with Openings, Subjected to Precompression", Designing, Engineering and Construction with Masonry Products, Edited by F. B. Johnson, Gulf Publishing Co., Houston, Texas, May 1969.

25. Frocht, M. M., Photoelasticity, John Wiley & Sons Inc., New York, 1941.

26. Stafford-Smith, B., Carter, C., and Choudhury, J. R., "The Diagonal Tensile Strength of Brickwork", The Structural Engineer, No. 4, Vol. 48, June 1970.

27. Priestley, M. J. N., "Seismic Resistance of Reinforced Concrete Masonry Shear Walls with High Steel Percentages", Bulletin of the New Zealand National Society for Earthquake Engineering, Vol. 10, No. 1, March 1977.

28. Mayes, R. L., and Clough, R. W., "State of the Art on Seismic Shear Strength of Masonry - An Evaluation and Review", EERC Report No. 75-21, University of California, Berkeley, October 1975.

29. Hegemier, G. A., "Mechanics of Reinforced Concrete Masonry: A Literature Survey", Report No. AMES-NSF TR-75-5-S, University of California, San Diego, 1975.

EARTHQUAKE ENGINEERING RESEARCH CENTER REPORTS

NOTE: Numbers in parenthesis are Accession Numbers assigned by the National Technical Information Service; these are followed by a price code. Copies of the reports may be ordered from the National Technical Information Service, 5285 Port Royal Road, Springfield, Virginia, 22161. Accession Numbers should be quoted on orders for reports (PB --- ---) and remittance must accompany each order. Reports without this information were not available at time of printing. Upon request, EERC will mail inquirers this information when it becomes available.

EERC 67-1 "Feasibility Study Large-Scale Earthquake Simulator Facility," by J. Penzien, J.G. Bouwkamp, R.W. Clough and D. Rea - 1967 (PB 187 905)A07

EERC 68-1 Unassigned

EERC 68-2 "Inelastic Behavior of Beam-to-Column Subassemblages Under Repeated Loading," by V.V. Bertero - 1968 (PB 184 888)A05

EERC 68-3 "A Graphical Method for Solving the Wave Reflection-Refraction Problem," by H.D. McNiven and Y. Mengi - 1968 (PB 187 943)A03

EERC 68-4 "Dynamic Properties of McKinley School Buildings," by D. Rea, J.G. Bouwkamp and R.W. Clough - 1968 (PB 187 902)A07

EERC 68-5 "Characteristics of Rock Motions During Earthquakes," by H.B. Seed, I.M. Idriss and F.W. Kiefer - 1968 (PB 188 338)A03

EERC 69-1 "Earthquake Engineering Research at Berkeley," - 1969 (PB 187 906)A11

EERC 69-2 "Nonlinear Seismic Response of Earth Structures," by M. Dibaj and J. Penzien - 1969 (PB 187 904)A08

EERC 69-3 "Probabilistic Study of the Behavior of Structures During Earthquakes," by R. Ruiz and J. Penzien - 1969 (PB 187 886)A06

EERC 69-4 "Numerical Solution of Boundary Value Problems in Structural Mechanics by Reduction to an Initial Value Formulation," by N. Distefano and J. Schujman - 1969 (PB 187 942)A02

EERC 69-5 "Dynamic Programming and the Solution of the Biharmonic Equation," by N. Distefano - 1969 (PB 187 941)A03

EERC 69-6 "Stochastic Analysis of Offshore Tower Structures," by A.K. Malhotra and J. Penzien - 1969 (PB 187 903)A09

EERC 69-7 "Rock Motion Accelerograms for High Magnitude Earthquakes," by H.B. Seed and I.M. Idriss - 1969 (PB 187 940)A02

EERC 69-8 "Structural Dynamics Testing Facilities at the University of California, Berkeley," by R.M. Stephen, J.G. Bouwkamp, R.W. Clough and J. Penzien - 1969 (PB 189 111)A04

EERC 69-9 "Seismic Response of Soil Deposits Underlain by Sloping Rock Boundaries," by H. Dezfulian and H.B. Seed 1969 (PB 189 114)A03

EERC 69-10 "Dynamic Stress Analysis of Axisymmetric Structures Under Arbitrary Loading," by S. Ghosh and E.L. Wilson 1969 (PB 189 026)A10

EERC 69-11 "Seismic Behavior of Multistory Frames Designed by Different Philosophies," by J.C. Anderson and V. V. Bertero - 1969 (PB 190 662)A10

EERC 69-12 "Stiffness Degradation of Reinforcing Concrete Members Subjected to Cyclic Flexural Moments," by V.V. Bertero, B. Bresler and H. Ming Liao - 1969 (PB 202 942)A07

EERC 69-13 "Response of Non-Uniform Soil Deposits to Travelling Seismic Waves," by H. Dezfulian and H.B. Seed - 1969 (PB 191 023)A03

EERC 69-14 "Damping Capacity of a Model Steel Structure," by D. Rea, R.W. Clough and J.G. Bouwkamp - 1969 (PB 190 663)A06

EERC 69-15 "Influence of Local Soil Conditions on Building Damage Potential during Earthquakes," by H.B. Seed and I.M. Idriss - 1969 (PB 191 036)A03

EERC 69-16 "The Behavior of Sands Under Seismic Loading Conditions," by M.L. Silver and H.B. Seed - 1969 (AD 714 982)A07

EERC 70-1 "Earthquake Response of Gravity Dams," by A.K. Chopra - 1970 (AD 7[illegible] 640)A03

EERC 70-2 "Relationships between Soil Conditions and Building Damage in the Caracas Earthquake of July 29, 1967," by H.B. Seed, I.M. Idriss and H. Dezfulian - 1970 (PB 195 762)A05

EERC 70-3 "Cyclic Loading of Full Size Steel Connections," by E.P. Popov and R.M. Stephen - 1970 (PB 213 545)A04

EERC 70-4 "Seismic Analysis of the Charaima Building, Caraballeda, Venezuela," by Subcommittee of the SEAONC Research Committee: V.V. Bertero, P.F. Fratessa, S.A. Mahin, J.H. Sexton, A.C. Scordelis, E.L. Wilson, L.A. Wyllie, H.B. Seed and J. Penzien, Chairman - 1970 (PB 201 455)A06

EERC 70-5 "A Computer Program for Earthquake Analysis of Dams," by A.K. Chopra and P. Chakrabarti - 1970 (AD 723 994)A05

EERC 70-6 "The Propagation of Love Waves Across Non-Horizontally Layered Structures," by J. Lysmer and L.A. Drake 1970 (PB 197 896)A03

EERC 70-7 "Influence of Base Rock Characteristics on Ground Response," by J. Lysmer, H.B. Seed and P.B. Schnabel 1970 (PB 197 897)A03

EERC 70-8 "Applicability of Laboratory Test Procedures for Measuring Soil Liquefaction Characteristics under Cyclic Loading," by H.B. Seed and W.H. Peacock - 1970 (PB 198 016)A03

EERC 70-9 "A Simplified Procedure for Evaluating Soil Liquefaction Potential," by H.B. Seed and I.M. Idriss - 1970 (PB 198 009)A03

EERC 70-10 "Soil Moduli and Damping Factors for Dynamic Response Analysis," by H.B. Seed and I.M. Idriss - 1970 (PB 197 869)A03

EERC 71-1 "Koyna Earthquake of December 11, 1967 and the Performance of Koyna Dam," by A.K. Chopra and P. Chakrabarti 1971 (AD 731 496)A06

EERC 71-2 "Preliminary In-Situ Measurements of Anelastic Absorption in Soils Using a Prototype Earthquake Simulator," by R.D. Borcherdt and P.W. Rodgers - 1971 (PB 201 454)A03

EERC 71-3 "Static and Dynamic Analysis of Inelastic Frame Structures," by F.L. Porter and G.H. Powell - 1971 (PB 210 135)A06

EERC 71-4 "Research Needs in Limit Design of Reinforced Concrete Structures," by V.V. Bertero - 1971 (PB 202 943)A04

EERC 71-5 "Dynamic Behavior of a High-Rise Diagonally Braced Steel Building," by D. Rea, A.A. Shah and J.G. Bouwkamp 1971 (PB 203 584)A06

EERC 71-6 "Dynamic Stress Analysis of Porous Elastic Solids Saturated with Compressible Fluids," by J. Ghaboussi and E. L. Wilson - 1971 (PB 211 396)A06

EERC 71-7 "Inelastic Behavior of Steel Beam-to-Column Subassemblages," by H. Krawinkler, V.V. Bertero and E.P. Popov 1971 (PB 211 335)A14

EERC 71-8 "Modification of Seismograph Records for Effects of Local Soil Conditions," by P. Schnabel, H.B. Seed and J. Lysmer - 1971 (PB 214 450)A03

EERC 72-1 "Static and Earthquake Analysis of Three Dimensional Frame and Shear Wall Buildings," by E.L. Wilson and H.H. Dovey - 1972 (PB 212 904)A05

EERC 72-2 "Accelerations in Rock for Earthquakes in the Western United States," by P.B. Schnabel and H.B. Seed - 1972 (PB 213 100)A03

EERC 72-3 "Elastic-Plastic Earthquake Response of Soil-Building Systems," by T. Minami - 1972 (PB 214 868)A08

EERC 72-4 "Stochastic Inelastic Response of Offshore Towers to Strong Motion Earthquakes," by M.K. Kaul - 1972 (PB 215 713)A05

EERC 72-5 "Cyclic Behavior of Three Reinforced Concrete Flexural Members with High Shear," by E.P. Popov, V.V. Bertero and H. Krawinkler - 1972 (PB 214 555)A05

EERC 72-6 "Earthquake Response of Gravity Dams Including Reservoir Interaction Effects," by P. Chakrabarti and A.K. Chopra - 1972 (AD 762 330)A08

EERC 72-7 "Dynamic Properties of Pine Flat Dam," by D. Rea, C.Y. Liaw and A.K. Chopra - 1972 (AD 763 928)A05

EERC 72-8 "Three Dimensional Analysis of Building Systems," by E.L. Wilson and H.H. Dovey - 1972 (PB 222 438)A06

EERC 72-9 "Rate of Loading Effects on Uncracked and Repaired Reinforced Concrete Members," by S. Mahin, V.V. Bertero, D. Rea and M. Atalay - 1972 (PB 224 520)A08

EERC 72-10 "Computer Program for Static and Dynamic Analysis of Linear Structural Systems," by E.L. Wilson, K.-J. Bathe, J.E. Peterson and H.H.Dovey - 1972 (PB 220 437)A04

EERC 72-11 "Literature Survey - Seismic Effects on Highway Bridges," by T. Iwasaki, J. Penzien and R.W. Clough - 1972 (PB 215 613)A19

EERC 72-12 "SHAKE-A Computer Program for Earthquake Response Analysis of Horizontally Layered Sites," by P.B. Schnabel and J. Lysmer - 1972 (PB 220 207)A06

EERC 73-1 "Optimal Seismic Design of Multistory Frames," by V.V. Bertero and H. Kamil - 1973

EERC 73-2 "Analysis of the Slides in the San Fernando Dams During the Earthquake of February 9, 1971," by H.B. Seed, K.L. Lee, I.M. Idriss and F. Makdisi - 1973 (PB 223 402)A14

EERC 73-3 "Computer Aided Ultimate Load Design of Unbraced Multistory Steel Frames," by M.B. El-Hafez and G.H. Powell 1973 (PB 248 315)A09

EERC 73-4 "Experimental Investigation into the Seismic Behavior of Critical Regions of Reinforced Concrete Components as Influenced by Moment and Shear," by M. Celebi and J. Penzien - 1973 (PB 215 884)A09

EERC 73-5 "Hysteretic Behavior of Epoxy-Repaired Reinforced Concrete Beams," by M. Celebi and J. Penzien - 1973 (PB 239 568)A03

EERC 73-6 "General Purpose Computer Program for Inelastic Dynamic Response of Plane Structures," by A. Kanaan and G.H. Powell - 1973 (PB 221 260)A08

EERC 73-7 "A Computer Program for Earthquake Analysis of Gravity Dams Including Reservoir Interaction," by P. Chakrabarti and A.K. Chopra - 1973 (AD 766 271)A04

EERC 73-8 "Behavior of Reinforced Concrete Deep Beam-Column Subassemblages Under Cyclic Loads," by O. Küstü and J.G. Bouwkamp - 1973 (PB 246 117)A12

EERC 73-9 "Earthquake Analysis of Structure-Foundation Systems," by A.K. Vaish and A.K. Chopra - 1973 (AD 766 272)A07

EERC 73-10 "Deconvolution of Seismic Response for Linear Systems," by R.B. Reimer - 1973 (PB 227 179)A08

EERC 73-11 "SAP IV: A Structural Analysis Program for Static and Dynamic Response of Linear Systems," by K.-J. Bathe, E.L. Wilson and F.E. Peterson - 1973 (PB 221 967)A09

EERC 73-12 "Analytical Investigations of the Seismic Response of Long, Multiple Span Highway Bridges," by W.S. Tseng and J. Penzien - 1973 (PB 227 816)A10

EERC 73-13 "Earthquake Analysis of Multi-Story Buildings Including Foundation Interaction," by A.K. Chopra and J.A. Gutierrez - 1973 (PB 222 970)A03

EERC 73-14 "ADAP: A Computer Program for Static and Dynamic Analysis of Arch Dams," by R.W. Clough, J.M. Raphael and S. Mojtahedi - 1973 (PB 223 763)A09

EERC 73-15 "Cyclic Plastic Analysis of Structural Steel Joints," by R.B. Pinkney and R.W. Clough - 1973 (PB 226 843)A08

EERC 73-16 "QUAD-4: A Computer Program for Evaluating the Seismic Response of Soil Structures by Variable Damping Finite Element Procedures," by I.M. Idriss, J. Lysmer, R. Hwang and H.B. Seed - 1973 (PB 229 424)A05

EERC 73-17 "Dynamic Behavior of a Multi-Story Pyramid Shaped Building," by R.M. Stephen, J.P. Hollings and J.G. Bouwkamp - 1973 (PB 240 718)A06

EERC 73-18 "Effect of Different Types of Reinforcing on Seismic Behavior of Short Concrete Columns," by V.V. Bertero, J. Hollings, O. Küstü, R.M. Stephen and J.G. Bouwkamp - 1973

EERC 73-19 "Olive View Medical Center Materials Studies, Phase I," by B. Bresler and V.V. Bertero - 1973 (PB 235 986)A06

EERC 73-20 "Linear and Nonlinear Seismic Analysis Computer Programs for Long Multiple-Span Highway Bridges," by W.S. Tseng and J. Penzien - 1973

EERC 73-21 "Constitutive Models for Cyclic Plastic Deformation of Engineering Materials," by J.M. Kelly and P.P. Gillis 1973 (PB 226 024)A03

EERC 73-22 "DRAIN - 2D User's Guide," by G.H. Powell - 1973 (PB 227 016)A05

EERC 73-23 "Earthquake Engineering at Berkeley - 1973," (PB 226 033)A11

EERC 73-24 Unassigned

EERC 73-25 "Earthquake Response of Axisymmetric Tower Structures Surrounded by Water," by C.Y. Liaw and A.K. Chopra 1973 (AD 773 052)A09

EERC 73-26 "Investigation of the Failures of the Olive View Stairtowers During the San Fernando Earthquake and Their Implications on Seismic Design," by V.V. Bertero and R.G. Collins - 1973 (PB 235 106)A13

EERC 73-27 "Further Studies on Seismic Behavior of Steel Beam-Column Subassemblages," by V.V. Bertero, H. Krawinkler and E.P. Popov - 1973 (PB 234 172)A06

EERC 74-1 "Seismic Risk Analysis," by C.S. Oliveira - 1974 (PB 235 920)A06

EERC 74-2 "Settlement and Liquefaction of Sands Under Multi-Directional Shaking," by R. Pyke, C.K. Chan and H.B. Seed 1974

EERC 74-3 "Optimum Design of Earthquake Resistant Shear Buildings," by D. Ray, K.S. Pister and A.K. Chopra - 1974 (PB 231 172)A06

EERC 74-4 "LUSH - A Computer Program for Complex Response Analysis of Soil-Structure Systems," by J. Lysmer, T. Udaka, H.B. Seed and R. Hwang - 1974 (PB 236 796)A05

EERC 74-5 "Sensitivity Analysis for Hysteretic Dynamic Systems: Applications to Earthquake Engineering," by D. Ray 1974 (PB 233 213)A06

EERC 74-6 "Soil Structure Interaction Analyses for Evaluating Seismic Response," by H.B. Seed, J. Lysmer and R. Hwang 1974 (PB 236 519)A04

EERC 74-7 Unassigned

EERC 74-8 "Shaking Table Tests of a Steel Frame - A Progress Report," by R.W. Clough and D. Tang - 1974 (PB 240 869)A03

EERC 74-9 "Hysteretic Behavior of Reinforced Concrete Flexural Members with Special Web Reinforcement," by V.V. Bertero, E.P. Popov and T.Y. Wang - 1974 (PB 236 797)A07

EERC 74-10 "Applications of Reliability-Based, Global Cost Optimization to Design of Earthquake Resistant Structures," by E. Vitiello and K.S. Pister - 1974 (PB 237 231)A06

EERC 74-11 "Liquefaction of Gravelly Soils Under Cyclic Loading Conditions," by R.T. Wong, H.B. Seed and C.K. Chan 1974 (PB 242 042)A03

EERC 74-12 "Site-Dependent Spectra for Earthquake-Resistant Design," by H.B. Seed, C. Ugas and J. Lysmer - 1974 (PB 240 953)A03

EERC 74-13 "Earthquake Simulator Study of a Reinforced Concrete Frame," by P. Hidalgo and R.W. Clough - 1974 (PB 241 944)A13

EERC 74-14 "Nonlinear Earthquake Response of Concrete Gravity Dams," by N. Pal - 1974 (AD/A 006 583)A06

EERC 74-15 "Modeling and Identification in Nonlinear Structural Dynamics - I. One Degree of Freedom Models," by N. Distefano and A. Rath - 1974 (PB 241 548)A06

EERC 75-1 "Determination of Seismic Design Criteria for the Dumbarton Bridge Replacement Structure, Vol. I: Description, Theory and Analytical Modeling of Bridge and Parameters," by F. Baron and S.-H. Pang - 1975 (PB 259 407)A15

EERC 75-2 "Determination of Seismic Design Criteria for the Dumbarton Bridge Replacement Structure, Vol. II: Numerical Studies and Establishment of Seismic Design Criteria," by F. Baron and S.-H. Pang - 1975 (PB 259 408)A11 (For set of EERC 75-1 and 75-2 (PB 259 406))

EERC 75-3 "Seismic Risk Analysis for a Site and a Metropolitan Area," by C.S. Oliveira - 1975 (PB 248 134)A09

EERC 75-4 "Analytical Investigations of Seismic Response of Short, Single or Multiple-Span Highway Bridges," by M.-C. Chen and J. Penzien - 1975 (PB 241 454)A09

EERC 75-5 "An Evaluation of Some Methods for Predicting Seismic Behavior of Reinforced Concrete Buildings," by S.A. Mahin and V.V. Bertero - 1975 (PB 246 306)A16

EERC 75-6 "Earthquake Simulator Study of a Steel Frame Structure, Vol. I: Experimental Results," by R.W. Clough and D.T. Tang - 1975 (PB 243 981)A13

EERC 75-7 "Dynamic Properties of San Bernardino Intake Tower," by D. Rea, C.-Y. Liaw and A.K. Chopra - 1975 (AD/A008 406) A05

EERC 75-8 "Seismic Studies of the Articulation for the Dumbarton Bridge Replacement Structure, Vol. I: Description, Theory and Analytical Modeling of Bridge Components," by F. Baron and R.E. Hamati - 1975 (PB 251 539)A07

EERC 75-9 "Seismic Studies of the Articulation for the Dumbarton Bridge Replacement Structure, Vol. 2: Numerical Studies of Steel and Concrete Girder Alternates," by F. Baron and R.E. Hamati - 1975 (PB 251 540)A10

EERC 75-10 "Static and Dynamic Analysis of Nonlinear Structures," by D.P. Mondkar and G.H. Powell - 1975 (PB 242 434)A08

EERC 75-11 "Hysteretic Behavior of Steel Columns," by E.P. Popov, V.V. Bertero and S. Chandramouli - 1975 (PB 252 365)A11

EERC 75-12 "Earthquake Engineering Research Center Library Printed Catalog," - 1975 (PB 243 711)A26

EERC 75-13 "Three Dimensional Analysis of Building Systems (Extended Version)," by E.L. Wilson, J.P. Hollings and H.H. Dovey - 1975 (PB 243 989)A07

EERC 75-14 "Determination of Soil Liquefaction Characteristics by Large-Scale Laboratory Tests," by P. De Alba, C.K. Chan and H.B. Seed - 1975 (NUREG 0027)A08

EERC 75-15 "A Literature Survey - Compressive, Tensile, Bond and Shear Strength of Masonry," by R.L. Mayes and R.W. Clough - 1975 (PB 246 292)A10

EERC 75-16 "Hysteretic Behavior of Ductile Moment Resisting Reinforced Concrete Frame Components," by V.V. Bertero and E.P. Popov - 1975 (PB 246 388)A05

EERC 75-17 "Relationships Between Maximum Acceleration, Maximum Velocity, Distance from Source, Local Site Conditions for Moderately Strong Earthquakes," by H.B. Seed, R. Murarka, J. Lysmer and I.M. Idriss - 1975 (PB 248 172)A03

EERC 75-18 "The Effects of Method of Sample Preparation on the Cyclic Stress-Strain Behavior of Sands," by J. Mulilis, C.K. Chan and H.B. Seed - 1975 (Summarized in EERC 75-28)

EERC 75-19 "The Seismic Behavior of Critical Regions of Reinforced Concrete Components as Influenced by Moment, Shear and Axial Force," by M.B. Atalay and J. Penzien - 1975 (PB 258 842)A11

EERC 75-20 "Dynami. Properties of an Eleven Story Masonry Building," by R.M. Stephen, J. . Hollings, J.G. Bouwkamp and D. Jurukovski - 1975 (PB 246 945)A04

EERC 75-21 "State-of-the-Art in Seismic Strength of Masonry - An Evaluation and Review," by R.L. Mayes and R.W. Clough 1975 (PB 249 040)A07

EERC 75-22 "Frequency Dependent Stiffness Matrices for Viscoelastic Half-Pl. Foundations," by A.K. Chopra, P. Chakrabarti and G. Dasgupta - 1975 (PB 248 121)A07

EERC 75-23 "Hysteretic Behavior of Reinforced Concrete Framed Walls," by T.Y. Wong, V.V. Bertero and E.P. Popov - 1975

EERC 75-24 "Testing Facility for Subassemblages of Frame-Wall Structural Systems," by V.V. Bertero, E.P. Popov and T. Endo - 1975

EERC 75-25 "Influence of Seismic History on the Liquefaction Characteristics of Sands," by H.B. Seed, K. Mori and C.K. Chan - 1975 (Summarized in EERC 75-28)

EERC 75-26 "The Generation and Dissipation of Pore Water Pressures during Soil Liquefaction," by H.B. Seed, P.P. Martin and J. Lysmer - 1975 (PB 252 648)A03

EERC 75-27 "Identification of Research Needs for Improving Aseismic Design of Building Structures," by V.V. Bertero 1975 (PB 248 136)A05

EERC 75-28 "Evaluation of Soil Liquefaction Potential during Earthquakes," by H.B. Seed, I. Arango and C.K. Chan - 1975 (NUREG 0026)A13

EERC 75-29 "Representation of Irregular Stress Time Histories b· Equivalent Uniform Stress Series in Liquefaction Analyses," by H.B. Seed, I.M. Idriss, F. Makdisi and N. Banerjee - 1975 (PB 252 635)A03

EERC 75-30 "FLUSH - A Computer Program for Approximate 3-D Analysis of Soil-Structure Interaction Problems," by J. Lysmer, T. Udaka, C.-F. Tsai and H.B. Seed - 1975 (PB 259 332)A07

EERC 75-31 "ALUSH - A Computer Program for Seismic Response Analysis of Axisymmetric Soil-Structure Systems," by E. Berger, J. Lysmer and H.B. Seed - 1975

EERC 75-32 "TRIP and TRAVEL - Computer Programs for Soil-Structure Interaction Analysis with Horizontally Travelling Waves," by T. Udaka, J. Lysmer and H.B. Seed - 1975

"-33 "Predicting the Performance of Structures in Regions of High Seismicity," by J. Penzien - 1975 (PB 248 130)A03

EERC 75-34 "Efficient Finite Element Analysis of Seismic Structure - Soil - Direction," by J. Lysmer, H.B. Seed, T. Udaka, R.N. Hwang and C.-F. Tsai - 1975 (PB 253 570)A03

EERC 75-35 "The Dynamic Behavior of a First Story Girder of a Three-Story Steel Frame Subjected to Earthquake Loading," by R.W. Clough and L.-Y. Li - 1975 (PB 248 841)A05

EERC 75-36 "Earthquake Simulator Study of a Steel Frame Structure, Volume II - Analytical Results," by D.T. Tang - 1975 (PB 252 926)A10

EERC 75-37 "ANSR-I General Purpose Computer Program for Analysis of Non-Linear Structural Response," by D.P. Mondkar and G.H. Powell - 1975 (PB 252 386)A08

EERC 75-38 "Nonlinear Response Spectra for Probabilistic Seismic Design and Damage Assessment of Reinforced Concrete Structures," by M. Murakami and J. Penzien - 1975 (PB 259 530)A05

EERC 75-39 "Study of a Method of Feasible Directions for Optimal Elastic Design of Frame Structures Subjected to Earthquake Loading," by N.D. Walker and K.S. Pister - 1975 (PB 257 781)A06

EERC 75-40 "An Alternative Representation of the Elastic-Viscoelastic Analogy," by G. Dasgupta and J.L. Sackman - 1975 (PB 252 173)A03

EERC 75-41 "Effect of Multi-Directional Shaking on Liquefaction of Sands," by H.B. Seed, R. Pyke and G.R. Martin - 1975 (PB 258 781)A03

EERC 76-1 "Strength and Ductility Evaluation of Existing Low-Rise Reinforced Concrete Buildings - Screening Method," by T. Okada and B. Bresler - 1976 (PB 257 906)A11

EERC 76-2 "Experimental and Analytical Studies on the Hysteretic Behavior of Reinforced Concrete Rectangular and T-Beams," by S.-Y.M. Ma, E.P. Popov and V.V. Bertero - 1976 (PB 260 843)A12

EERC 76-3 "Dynamic Behavior of a Multistory Triangular-Shaped Building," by J. Petrovski, R.M. Stephen, E. Gartenbaum and J.G. Bouwkamp - 1976

EERC 76-4 "Earthquake Induced Deformations of Earth Dams," by N. Serff and H.B. Seed - 1976

EERC 76-5 "Analysis and Design of Tube-Type Tal' Building Structures," by H. de Clercq and G.H. Powell - 1976 (PB 252 220) A10

EERC 76-6 "Time and Frequency Domain Analysis of Three-Dimensional Ground Motions, San Fernando Earthquake," by T. Kubo and J. Penzien (PB 260 556)A11

EERC 76-7 "Expected Performance of Uniform Building Code Design Masonry Structures," by R.L. Mayes, Y. Omote, S.W. Chen and R.W. Clough - 1976

EERC 76-8 "Cyclic Shear Tests on Concrete Masonry Piers," Part I - Test Resul s," by R.L. Mayes, Y. Omote and R.W. Clough - 1976 (PB 264 424)A06

EERC 76-9 "A Substructure Method for Earthquake Analysis of Structure - Soil Interaction," by J.A. Gutierrez and A.K. Chopra - 1976 (PB 257 783)A08

EERC 76-10 "Stabilization of Potentially Liquefiable Sand Deposits using Gravel Drain Systems," by H.B. Seed and J.R. Booker - 1976 (PB 258 820)A04

EERC 76-11 "Influence of Design and Analysis Assumptions on Computed Inel.stic Response of Moderately Tall Frames," by G.H. Powell and D.G. Row - 1976

EERC 76-12 "Sensitivity Analysis for Hysteretic Dynamic Systems: Theory and Applications," by D. Ray, K.S. Pister and E. Polak - 1976 (PB 262 859)A04

EERC 76-13 "Coupled Lateral Torsional Response of Buildings to Ground Shaking," by C.L. Kan and A.K. Chopra - 1976 (PB 257 907)A09

EERC 76-14 "Seismic Analyses of the Banco de America," by V.V. Bertero, S.A. Mahin and J.A. Hollings - 1976

EERC 76-15 "Reinforced Concrete Frame 2: Seismic Testing and Analytical Correlation," by R.W. Clough and J. Gidwani - 1976 (PB 261 323)A08

EERC 76-16 "Cyclic Shear Tests on Masonry Piers, Part II - Analysis of Test Results," by R.L. Mayes, Y. Omote and R.W. Clough - 1976

For sale by the National Technical Information Service, U. S. Department of Commerce, Springfield, Virginia 22161.

See back of report for up to date listing of EERC reports.